# The $\iota(1440)$, anomalous Ward identities, and topological susceptibility for QCD

Peter Glyn Williams
*Physics Department, Queen Mary College, University of London, London E1 4NS England*
(Received 31 March 1986)

Anomalous Ward identities for QCD are comprehensively analyzed taking into account contributions of all known pseudoscalar mesons, including the $\iota(1440$ MeV) which is a possible glueball candidate. Implications for the standard resolution of the U(1) problem are examined by imposing the important and crucial constraint of positivity for the topological susceptibility. The pure Yang-Mills susceptibility—a quantity relevant in quenched lattice calculations—is shown to increase quite considerably in the presence of the $\iota$, while the total susceptibility is reduced and may even vanish. Allowed ranges for the axial couplings are delineated and two classes of solution emerge: one corresponding to an $\iota$ with suppressed singlet axial coupling; the other to a large $\eta'$-like coupling. It may be possible to discriminate between these two alternatives by measurements of the branching ratio for $\iota \to K\bar{K}\pi$: values near 100% give suppressed couplings; values below 50% unsuppressed ones.

## I. INTRODUCTION

The discovery of another low-lying pseudoscalar meson, the $\iota(1440)$ (Ref. 1), provides a possible candidate for one of the unique features of QCD: the glueball. The observed properties are not in contradiction with those of a glueball, although the apparent dominance by the so far only observed decay mode $\iota \to K\bar{K}\pi$ and its recently observed strong production in $\pi^- p$ scattering[2] both point to a strong $\bar{q}q$ admixture or radial excitation. Whether or not the iota is a glueball, its already established quantum numbers raise the important question of its role in the resolution of the U(1) problem[3] through the existence of gluons, their axial anomaly, and nonzero topological charge. When only the pseudoscalar nonet is invoked in their saturation the anomalous $U(3)\times U(3)$ Ward identities (WI's) of QCD provide a fairly successful phenomenology, including a resolution of the U(1) problem.[4,5] This success is considered to be evidence for the non-Abelian, topological aspects of the underlying theory. To reproduce these results from a truly fundamental calculation poses a most stringent test for QCD. Recent lattice Monte Carlo computations[6] in the pure Yang-Mills sector have successfully obtained a sufficiently large topological susceptibility $\chi_t^{\rm YM}$ and overcome the difficulties of previous attempts.[7] A full computation involving fermion loops is now desirable to demonstrate the large cancellation expected on very general grounds.[8] The existence and mass spectrum of glueballs also poses a difficult problem in lattice calculations[9] and their unambiguous experimental confirmation is even more problematic. It is therefore of considerable help to seek further tests both for QCD and for the phenomenological identification of glueball candidates. Here we present an attempt to evaluate the significance of the $\iota(1440)$ for QCD by examining its role in the saturation of the WI for the $U(3)\times U(3)$ chiral algebra. Because of our ignorance of the iota couplings and of the spectrum of $\bar{q}q$ radial excitations we have not been able to include the latter explicitly in the analysis; consequently our analysis can only be taken as illustrative of the effects of these higher-mass states on the U(1) problem and our topological interpretation of its resolution.

In this paper we show in detail how the iota affects the values of topological charge (the couplings $A_a$) and topological susceptibility obtained in previous analyses;[4,5] we find marked changes are possible, with the QCD susceptibility $\chi_t$ small, possibly even zero, and the "no quarks" susceptibility $\chi_t^{\rm YM}$ considerably enhanced. These results depend on the axial couplings of the iota which seem to favor an SU(3)-singlet identification. Whether the iota's singlet axial coupling is suppressed or not is correlated with the width for $\psi \to \iota\gamma$. Only the product of this width with the branching ratio for $\iota \to K\bar{K}\pi$ is currently measured[1,2] so that our conclusion depends on the latter branching ratio: values near 100%—at present more likely since other modes have been sought and not yet found[2]—favor a suppressed coupling.

Of course our conclusions depend on assumptions and approximations, particularly on the hope that the inclusion of the high-mass states does not vitiate the saturation approximation. In view of these reservations we also present a fairly comprehensive analysis of the dependence of the results on several experimental and theoretical uncertainties: with some provisos the conclusions are quite stable under these variations. The main limitation of this work is the neglect of so far unobserved $\bar{q}q$ radial excitations such as an $\eta$ expected at 1.7 GeV. This means that the "iota couplings" may not represent those of the iota itself but rather "effective" couplings of pseudoscalars above 1.4 GeV: the suppression referred to above is probably an indication that the iota and other states in that region are radial excitations; or more speculatively, it is at least consistent with the $1/\sqrt{N}$ suppression expected of a glueball iota. Unfortunately we cannot distinguish between the two possibilities with our present knowledge. Potentially significant uncertainties also lie in the extrapolation to the mass shell of the soft-meson current-algebra anomaly calculations for the two-photon widths of $\eta$, $\eta'$, and iota. We therefore make a serious attempt to assess these uncertainties and to avoid too much dependence on this part of the analysis. Despite this it turns out to be quite difficult to obtain a large $\iota \to 2\gamma$ width: our "best

 

bet" is $<2$ keV, although a value as large as 5 keV is not too difficult to arrange. Finally, it appears that the inclusion of the iota somewhat improves the overall fit to the data on the pseudoscalar mesons compared with analyses which excluded it.[4,5]

Our entire discussion is restricted to a domain of parameter space which is chosen to minimize deviations of $\eta$ and $\eta'$ couplings from SU(3) symmetry. We have been at pains to investigate a much wider range in our computations, and this information is presented in the many graphs in this paper. In general large deviations from SU(3) symmetry much beyond 20% are not favored by the sum rules for $2\gamma$ decays and the data on $\psi\to\iota\gamma$. Although it is common in the literature to assume SU(3) symmetry for $\eta$ and $\eta'$ couplings (see all the papers in Ref. 4 except for the last one), it is obviously not consistent with the little data that exists; but the extant data, often expressed in terms of a small $(-10°)$ $\eta-\eta'$ mixing angle[5] is consistent with deviations no larger than the 20% exhibited in the kaon axial coupling. This assumption is also consistent with the very sparse data on strong-interaction couplings of $\eta$ and $\eta'$ (Ref. 11).

Several previous investigations have covered some of these questions using similar or equivalent techniques.[12,13] The first[12] studied the pseudoscalar mass matrix and mixing with a phenomenological Lagrangian extended to include a *glueball* $\iota$, but with a very different philosophy especially regarding the input parameters, and without an exhaustive use of U(3)×U(3) Ward identities. This makes it difficult to give a detailed comparison with our work. The second paper[13] uses basically the same framework as we do, but fails to take account of the large Yang-Mills topological susceptibility in saturating the anomalous Ward identities and is therefore not self-consistent—see Ref. 14 for a detailed account of this disagreement. One consequence is that solutions could only be found in Ref. 13 with a branching ratio for $\iota\to K\bar{K}\pi\leq 30\%$. Here we show that this restriction is not required; on the contrary, although ratios as small as 30% are allowed there are also solutions with a branching ratio as large as 100%, consistent with experiment.[1] One common feature of our work and that of Refs. 12 and 13 (see also Ref. 15) is the prediction of a small $\iota\to 2\gamma$ width less than 5 keV; we show that this is perhaps not too surprising because it follows primarily from approximate SU(3) symmetry and the sum rules for the $2\gamma$ decays of $\eta$, $\eta'$, and $\iota$. An important new feature of this analysis (see also Ref. 14) is that we restrict the total topological susceptibility to be positive, a requirement not guaranteed by the saturated Ward identities themselves and one which leads to a crucial limitation on otherwise free parameters.

In Sec. II we present the WI's and our basic definitions and show how to include the effect of vacuum SU(3) breaking and the $\iota(1440)$; Sec. III follows with a critical analysis of the role of topological susceptibility in the WI's and is illustrated by the special case of SU(3) symmetry in Sec. IV to bring out clearly the effects of the iota and the importance of positivity restrictions. Section V discusses the additional experimental and theoretical input necessary for solving the WI's. Section VI presents a new general method for solving the WI's in the presence of the iota based on our previous work,[5] and is followed by Secs. VII and VIII where some remarkably simple expressions are given for the topological susceptibility. Finally Sec. IX presents our detailed numerical results followed by a concluding discussion in Sec. X. The Appendix deals with the interesting side issue of sign ambiguities and their resolution.

## II. ANOMALOUS WARD IDENTITIES

Quantum chromodynamics provides a concrete realization of the assumptions of the current algebra of chiral U(3)×U(3). Explicit symmetry breaking is supposed to arise from the quark masses $m\simeq m_u\simeq m_d$ and $m_s$; spontaneous breaking of chiral symmetry from nonzero quark correlation functions in the approximately SU(3)-symmetric vacuum $\langle\bar{u}u\rangle\simeq\langle\bar{d}d\rangle\neq 0$ and $\langle\bar{s}s\rangle\neq 0$. This spontaneous breaking is accompanied by a nonet of would-be Goldstone pseudoscalar bosons $\Pi_a(\pi,K,\eta,\eta')$ which have nonzero matrix elements to the vacuum when acted on by the divergence of the axial-vector currents:

$$\langle 0\,|\,\partial^\mu A^i_\mu(0)\,|\,\Pi_a\rangle = m_a{}^2 F_{ia},\quad i=0,\ldots,8\ . \tag{1}$$

In QCD the ninth axial-vector current and the corresponding meson play a special role by virtue of the existence of the gluon anomaly:

$$\partial^\mu A^i_\mu(x)=\bar{q}\gamma_5\frac{\lambda_i}{2}q+\delta_{i0}G\tilde{G}(x)\ , \tag{2}$$

where

$$G\tilde{G}\equiv\frac{\sqrt{3}}{\sqrt{2}}\frac{g^2}{16\pi^2}\frac{1}{2}\epsilon^{\mu\nu\alpha\beta}G^i_{\mu\nu}G^i_{\alpha\beta}=\partial^\mu K_\mu\ . \tag{3}$$

While the octet become massless Goldstone bosons in the chiral limit of vanishing quark masses, the ninth meson ($\eta'$) which is the would-be Goldstone boson of $U_A(1)$ keeps a mass through the anomaly as a consequence of its proportionality to the topological charge density—nonzero in QCD. This is measured by the topological charge constant of the $\eta'$ (and through mixing the $\eta$):

$$\langle 0\,|\,G\tilde{G}(0)\,|\,\Pi_a\rangle = m_a{}^2 A_a,\quad a=\eta,\eta'\ . \tag{4}$$

Only in the limit of infinitely many colors $N\to\infty$ do the anomaly and topological charge vanish and make the $\eta'$ a genuine $U_A(1)$ Goldstone boson. This is the solution of the so-called U(1) problem and provides an especially powerful test for the non-Abelian nature of QCD (Ref. 5).

This beautiful sequence of argumentation may be concretely expressed in terms of the anomalous Ward identities obtained for zero momentum vacuum expectation values of products of pairs of axial-vector current divergences as well as the anomaly itself. When saturated with the nonet of pseudoscalars and upon elimination of the quark masses and vacuum correlation functions these Ward identities give four sum rules:[5]

$$m_a{}^2 F_{8a}{}^2=\tfrac{1}{3}(4m_K{}^2F_K{}^2-m_\pi{}^2F_\pi{}^2)\ , \tag{5a}$$

$$m_a{}^2 F_{8a}F_{0a}=-\tfrac{2}{3}\sqrt{2}(m_K{}^2F_K{}^2-m_\pi{}^2F_\pi{}^2)\ , \tag{5b}$$

$$m_a{}^2F_{0a}(F_{0a}-A_a)=\tfrac{1}{3}(2m_K{}^2F_K{}^2+m_\pi{}^2F_\pi{}^2)\ , \tag{5c}$$

$$m_a{}^2F_{8a}A_a=0\ , \tag{5d}$$

where the repeated index $a$ is summed over $\eta$ and $\eta'$. Solutions to these equations (supplemented with judiciously chosen input) show that both $A_\eta$ and $A_{\eta'}$ are nonzero and of the order of $F_\pi$ in the real world, and therefore provide evidence for gluons, their anomaly, and QCD topological charge.[4,5] As they stand Eqs. (5) assume an SU(3)-symmetric vacuum state: $\langle\bar{u}u\rangle=\langle\bar{d}d\rangle=\langle\bar{s}s\rangle$. It is well known[16] that octet symmetry breaking in the vacuum $\langle\bar{s}s\rangle\neq\langle\bar{d}d\rangle$ leads to a very simple modification of (5) in which the measured $F_K$ is simply replaced by an "effective" $\bar{F}_K$ given by

$$m_K{}^2\bar{F}_K{}^2=m_K{}^2F_K{}^2-\frac{3}{2}\left[\left[\frac{m_s}{m}-1\right]\left[1-\frac{\langle\bar{s}s\rangle}{\langle\bar{u}u\rangle}\right]\right]\times\left[\left[\frac{m_s}{m}+2\right]\left[2+\frac{\langle\bar{s}s\rangle}{\langle\bar{u}u\rangle}\right]\right]^{-1}\ . \tag{5e}$$

Experimentally, $F_K=1.22\pm0.01$ in $F_\pi$ units[17] while estimates of vacuum symmetry breaking cover a wide range.[18] We take as typical the value[18a]

$$\frac{\langle\bar{s}s\rangle}{\langle\bar{u}u\rangle}\approx0.8\ \text{ with }\ \frac{m_s}{m}\approx36\ . \tag{5f}$$

This gives $\bar{F}_K\simeq1.1\pm0.5$ a value we use throughout this paper; the "error" is our own very conservative estimate of the theoretical range of disagreement. To avoid rewriting all our expressions with additional typographical complications we will use the symbol $F_K$ to stand for the octet breaking corrected quantity $\bar{F}_K$ defined by (5e).

The discovery of the $\iota(1440)$ makes it necessary either to include it in the summation on the left-hand sides of (5) or to justify its neglect. The $1/N$ expansion suggests that the couplings of a pure unmixed glueball are reduced by a factor of order $1/\sqrt{N}$ relative to the $\bar{q}q$ mesons; and $\bar{q}q$ radial excitations are also expected to be suppressed. Since we are largely ignorant of the $\iota(1440)$ couplings we are forced either to abandon the use of (5) or include the new meson without assuming that it has suppressed couplings. We may also ask whether it could play the role previously attributed to the $\eta,\eta'$ topological charge in solving the $U_A(1)$ problem without recourse to topology or gluon anomaly. In subsequent sections we show that the answer to this question is a fairly decisive no, and furthermore that the iota couplings are sufficiently constrained to provide evidence that they are indeed suppressed.

## III. TOPOLOGICAL SUSCEPTIBILITY

Crucial to our discussion will be a fifth Ward identity [Eq. (17)] for the topological susceptibility $\chi_t$, which measures $\theta$ dependence in the vacuum:

$$\chi_t=-\left[\frac{d^2E_{\text{vac}}}{d\theta^2}\right]_{\theta=0}=-\frac{i}{6}\int d^4x\,\partial^\mu\partial^\nu T\langle0\,|\,K_\mu(x)K_\nu(0)\,|\,0\rangle\ . \tag{6a}$$

In Crewther's notation[3] $\chi_t=\langle\langle\nu\rangle\rangle^2$; and in order to conform with the notation now being used in the lattice computations[6] is six times smaller than the $\chi_t$ used in our previous work.[14] This explains the awkward factors of 6 which appear frequently in this section; the *natural* definition would appear to be our original one[14] since it is the quantity to be compared with $m_\pi{}^2F_\pi{}^2$ [see Eqs. (40) and (41)]. As emphasized by Crewhter,[3,19] (6a) is the correct ambiguity-free *definition* of the squared topological density rather than the naive quantity:

$$\langle Q^2\rangle=-i\int d^4x\,T\langle0\,|\,G\tilde{G}(0)G\tilde{G}(0)\,|\,0\rangle\ . \tag{6b}$$

The latter time-ordered product of hard dimension-4 operators is not well defined because it contains $\delta$-function ambiguities which are removed by the definition (6a).

In a path-integral formulation we may write

$$\chi_t=Z^{-1}(0)\sum_\nu\nu^2Z_\nu(0)\ , \tag{7a}$$

where

$$Z(\theta)=\sum_\nu Z_\nu(\theta) \tag{7b}$$

and $Z_\nu(\theta)$ is the generating functional in which the integrated gluon fields have fixed winding number $\nu$. In the Euclidean domain (7a) is obviously positive, a property which continues into Minkowski space-time and which is respected by WKB calculations.[19] The positivity of $\chi_t$ is a crucial restriction in this paper; it bears on the present discussion because a naive saturation of either (6a) or (6b) with mesons not only leads to a negative-definite result, $-m_a{}^2A_a{}^2$, but gives the same value for both forms (6). Provided $A_a\neq0$, these negative terms are undoubtedly present; but obviously there must be something missing to guarantee positivity, at least for (6a). There are several equivalent ways to look at the extra term.

(i) Because one is dealing with operators of high dimension, any dispersion relation for $\chi_t$ would almost certainly require a *subtraction*, $\chi_t^0$, and lead to the general expression

$$6\chi_t=6\chi_t^0-m_a{}^2A_a{}^2\ . \tag{8}$$

This is a further unknown parameter which must be determined from positivity and the Ward identities.

(ii) Since the subtraction introduced in (8) must have the opposite sign to the contribution of physical mesons, it may be interpreted as the contribution of a negative-metric ghost state—the Kogut-Susskind mechanism. This appears rather naturally in the phenomenological Lagrangian approach[4] when the gluon operator $G\tilde{G}$ is incorporated with the pseudoscalars in an effective low-energy dynamics satisfying the Ward identities at each order of perturbation theory. In this formulation it is also ap-

parent that $\chi_t^0$ is a product of the pure gluon Yang-Mills sector.

(iii) A possible expression for $\chi_t^0$ as a contact term has been given by an argument due to Witten.[8] The idea is to run the derivatives in (6a) through the time ordering, picking up equal-time commutators which are evaluated in the canonical formalism in the temporal gauge $A_0=0$. The formal result is[4]

$$6\chi_t=\left[\frac{g^2}{8\pi^2}\right]^2\langle 0\,|\,\mathrm{Tr}\mathbf{B}^2(0)\,|\,0\rangle+\langle Q^2\rangle\ , \tag{9}$$

where $\mathbf{B}$ is the gluon color-magnetic field. If we assume saturation is permitted in (6a) but not in (6b) then we may identify

$$6\chi_t^2=\left[\frac{g^2}{8\pi^2}\right]^2\langle 0\,|\,\mathrm{Tr}\mathbf{B}^2\,|\,0\rangle\ . \tag{10}$$

The difficulty with this argument is that the intermediate steps are not justified because they involve unregularized quantities although it may well be that ambiguities actually cancel in the final expression (9). It does at least indicate how the subtraction in (8) may arise.

(iv) The final argument is a modified version of one given originally by Witten,[8] and starts with a pure Yang-Mills version of QCD in the absence of quarks having a vacuum with $\theta$ dependence:

$$\chi_t^{\mathrm{YM}}\equiv-\left[\frac{d^2E_{\mathrm{vac}}}{d\theta^2}\right]^{\theta=0}_{\text{no quarks}}\ . \tag{11}$$

In contrast with Witten we will not assume that $\chi_t^{\mathrm{YM}}\neq 0$, but will deduce it. Now consider QCD with at least one zero-mass quark. This theory has a $U_A(1)$ symmetry which by a suitable $\gamma_5$ transformation on the zero-mass quarks transforms away the $\theta$ dependence:

$$\chi_t\equiv-\left[\frac{d^2E_{\mathrm{vac}}}{d\theta^2}\right]^{\theta=0}_{m=0\text{ quarks}}=0\ . \tag{12}$$

Since in general this will have the form

$$\chi_t=\chi_t^{\mathrm{YM}}+(\bar{q}q\text{ meson contributions}) \tag{13}$$

and since by our previous arguments the meson contributions are negative definite, they must exactly cancel $\chi_t^{\mathrm{YM}}$ in the $m\to 0$ limit; assuming they are nonzero in this limit then shows that $\chi_t^{\mathrm{YM}}\neq 0$. We gave the argument in this form because it precisely mimics the way we solve the WI's: first by solving (5), thereby showing that the meson contributions to $\chi_t$ are indeed nonzero (i.e., $A_a\neq 0$), hence computing $\chi_t$ from a further WI (18) to be discussed shortly and finally obtaining $\chi_t^0$ from its defining Eq. (8).

There is yet another subtlety we must consider because it affects the interpretation of our final results: the relation between $\chi_t^{\mathrm{YM}}$ and $\chi_t^0$ is in general nontrivial since we expect at least one pseudoscalar glueball "$g$" even in the pure Yang-Mills theory, and this physical state would contribute negatively:

$$6\chi_t^{\mathrm{YM}}=6\chi_t^0-m_g{}^2A_g{}^2\ . \tag{14}$$

However, it is not possible to identify $g$ with $\iota(1440)$ even if the latter were a glueball since it would certainly have a considerable admixture of $\bar{q}q$; so the practical identification of $\chi_t^{\mathrm{YM}}$ is ambiguous even if we knew all the parameters appearing in (8). In practice we can probably only bound $\chi_t^{\mathrm{YM}}$ somewhere between the two extremes where there is no glueball component at all and where $\iota(1440)$ is a pure glueball:

$$6\chi_t^0-m_\iota{}^2A_\iota{}^2<6\chi_t^{\mathrm{YM}}\leq 6\chi_t^0\ . \tag{15}$$

The Ward identity leading to a determination of $\chi_t^0$ and $\chi_t$ may be obtained[5] from the vanishing of the following gauge-invariant $T$ product in the absence of massless pseudoscalar singlets:

$$\lim_{q\to 0}\int d^4x\,e^{iq\cdot x}\partial^\mu\partial^\nu T\langle 0\,|\,A_\mu^0(x)K_\nu(0)\,|\,0\rangle=0\ . \tag{16}$$

This leads to

$$6\chi_t=i\int d^4x\,T\langle 0\,|\,\partial_\mu\tilde{A}_\mu^{\,0}(x)G\tilde{G}(0)\,|\,0\rangle\ , \tag{17}$$

where $\partial_\mu\tilde{A}_\mu^{\,0}$ is the soft $\bar{q}\gamma_5 q$ part of the divergence in (2). Saturation of the right-hand side then gives

$$6\chi_t=m_a{}^2F_{0a}A_a-m_a{}^2A_a{}^2 \tag{18a}$$

$$=m_a{}^2(F_{0a}{}^2-A_a{}^2)-\tfrac{1}{3}(2m_K{}^2F_K{}^2+m_\pi{}^2F_\pi{}^2) \tag{18b}$$

from which we deduce, using (8),

$$6\chi_t^0=m_a{}^2F_{0a}A_a \tag{19a}$$

$$=m_a{}^2F_{0a}{}^2-\tfrac{1}{3}(2m_K{}^2F_K{}^2+m_\pi{}^2F_\pi{}^2)\ . \tag{19b}$$

In both cases the second form follows from using Eq. (5c).

Finally we note that although the form (18) is not obviously guaranteed to be positive because it depends on the sign of $(F_{0a}-A_a)$, nevertheless it is when only $\eta$ and $\eta'$ contribute by virtue of the Ward identities (5) [see Sec. VII, Eq. (40)]. However there is no longer the case when a third meson such as the $\iota(1440)$ is included, and this sets bounds on the magnitude of $(F_{0a}-A_a)$ which we can exploit.

## IV. THE SU(3)-SYMMETRIC CASE

Before attempting to study solutions to the Ward identities in detail it is useful first to examine a simple—possibly hypothetical—situation where iota is taken as a pure flavor-singlet glueball ($\iota=g$) and the axial couplings are SU(3) symmetric:

$$F_{8\eta'}=F_{0\eta}=0=F_{8g},\quad F_{0\eta'}=F_{8\eta}=F_\pi=F_K\approx 2F_{0g}\ . \tag{20}$$

The $1/N$ expansion suggests that $F_{0g}\sim O(1/\sqrt{N})F_\pi\sim\frac{1}{2}F_\pi$ for SU(3); we use this value for illustration only and keep $F_{0g}$ explicit in all the equations. The saturated Ward identities (5) lead in $F_\pi$ units to

$$m_K=m_\pi\ , \tag{21a}$$

$$m_\eta=m_\pi\ , \tag{21b}$$

$$A_\eta=0\ , \tag{21c}$$

and

$$m_{\eta'}{}^2=\frac{m_\pi{}^2-m_g{}^2F_{0g}(F_{0g}-A_g)}{(1-A_{\eta'})}\ . \tag{21d}$$

The first three equations are an obvious consequence of SU(3) symmetry; the last expresses the $U_A(1)$ problem and its solution succinctly, at least when the glueball is absent: the dynamical enhancement of the $\eta'$ mass over that of the pion is achieved by a topological charge constant $A_{\eta'}\simeq O(F_\pi)$ to give a small denominator. How does the presence of the glueball term change this picture? A large glueball mass $m_g\sim 1.4\ \text{GeV}\gg m_\pi$ is a consequence of both lattice[9] and bag[20] calculations. Since these are pure Yang-Mills flavor-symmetric models, this is probably the appropriate scale of glueball mass to use in (21d). It would appear therefore, that a nonzero $A_{\eta'}$ is no longer required: the large $\eta'$ mass could result from the glueball mass term in the numerator of (21d) *provided* $A_g$ is large enough to change the sign of this term. Thus, to obtain an enhanced $\eta'$ mass, say $m_{\eta'}\approx\frac{1}{2}m_g$ with the choice $A_{\eta'}=0$ would require $A_g\simeq F_\pi$; the enhancement now comes entirely from the glueball mass scale, but still requires topological charge; in the case of the glueball in order to reverse the sign of its contribution in (21d). Clearly there are intermediate possibilities with $A_{\eta'}$ and $A_g$ both nonvanishing. The opposite extreme with a small denominator providing an enhancement of the pion mass requires a suppression of the glueball term: $A_g\approx\frac{1}{2}F_\pi\approx F_{0g}$. In all cases we observe the essential role played by the topological charge: at least one of $A_{\eta'}$ and $A_g$ must be present. The fact that only the last mentioned scenario—$A_g\approx F_{0g}$—is possible now follows from the requirement that the topological susceptibility $\chi_t$ be positive:

$$6\chi_t=m_{\eta'}{}^2A_{\eta'}(1-A_{\eta'})+m_g{}^2F_{0g}(F_{0g}-A_g)$$

$$\simeq m_{\eta'}{}^2\left[(1-A_{\eta'})\left[A_{\eta'}-\frac{A_g}{F_{0g}}\right]+\left[\frac{m_\pi}{m_{\eta'}}\right]^2\frac{A_g}{F_{0g}}\right]\geq 0\ , \tag{22}$$

where the first line follows from (18a); the second from substituting (21d) to eliminate the glueball mass. In the chiral limit $m_\pi=0$ the last term is absent and the boundaries of positive $\chi_t$ are two intersecting straight lines enclosing the allowed single-hatched region $2A_g\geq A_{\eta'}\geq F_\pi$ in Fig. 1(a). Since the last term is not negligible—we are not in the full chiral limit $m_\pi=0$—in fact the boundaries are nonintersecting curves asymptotic to the chiral limit lines and separated at their nearest point $A_g=F_{0g}$ by $2m_\pi/m_{\eta'}$; this is the single-hatched region in Fig. 1(b). Lines of constant $m_{\eta'}$ given by (21d) intersect this region over a very limited range of $A_g$ and $A_{\eta'}$ [$A_g\approx F_{0g}\pm 0.1F_\pi$, $A_{\eta'}\approx(1\pm 0.2)F_\pi$] which clearly favors the mechanism of dynamical enhancement of the $\eta'$ mass with a suppression of the glueball contribution in (21d) through the near equality of $A_g$ and $F_{0g}$. For fixed $m_\pi, m_g$ the region of positive $\chi_t$ increases as $m_{\eta'}$ is reduced until at $m_{\eta'}=m_g$ this region is bounded by the $A_{\eta'}$ axis and a straight line crossing the axis at $A_{\eta'}=1$ and passing through the point $A_{\eta'}=2$, $A_g=F_{0g}$; the line $m_g=m_\pi$ is now a very nearly horizontal one at $A_g=F_{0g}$. This is the opposite extreme to the physical solution, allowing $A_{\eta'}$ to have a value anywhere between 0 and 2, but with $A_g\simeq F_{0g}$ throughout this range. Thus we see that nowhere is it possible to have *both* $A_g$ and $A_{\eta'}$ zero (unless, of course, $F_{0g}=0$): whatever the mechanism for generating the $\eta'$ mass we are driven to nontrivial topological effects.

All the ingredients of this discussion will feature importantly in the sequel with the additional complication of SU(3)-symmetry breaking and the consequent quite im-

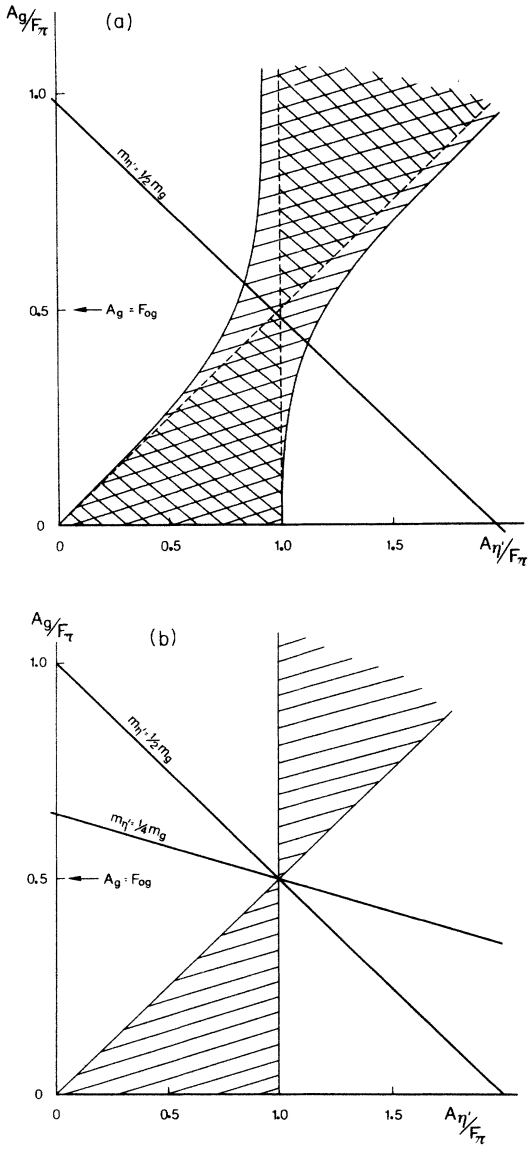


FIG. 1. (a) Regions of positive topological susceptibility with SU(3) symmetry for a pure singlet glueball iota ($\iota=g$) are shown single hatched; the chiral limit is shown double hatched. A line of fixed glueball mass is shown to illustrate the narrow allowed range of couplings. (b) Same as (a), but in the chiral limit $m_\pi\to 0$.

portant effects of mixing between the three pseudoscalar states. Note especially that the mechanism driving $A_g$ toward $F_{0g}$ does not depend on the fact that $m_g \gg m_{\eta'}$ but only on $m_\pi \ll m_g$ and $m_{\eta'}$.

## V. SUPPLEMENTING THE WARD IDENTITIES

To solve the Ward identities (5) in the general case we extend a method developed in our earlier investigations.[5] Since there are only four equations (5a)–(5d), but nine unmeasured quantities $(F_{8a},F_{0a},A_a;a=\eta,\eta',\iota)$ it is not possible to find a unique solution. Several independent additional conditions may be imposed to narrow down the choice.

(1) Gluon operator dominance of the radiative decays $\Psi\to\Pi_a\gamma(\Pi_a=\eta,\eta',\iota)$ provide two constraints:

$$R_{\eta'/\eta}\equiv\left[\frac{\Gamma(\psi\to\eta'\gamma)}{\Gamma(\psi\to\eta\gamma)}\frac{p_\eta{}^3}{p_{\eta'}{}^3}\right]^{1/2}\left[\frac{m_\eta}{m_{\eta'}}\right]^2=\frac{A_{\eta'}}{A_\eta} \tag{23a}$$

and

$$R_{\eta'/\iota}\equiv\left[\frac{\Gamma(\psi\to\eta'\gamma)}{\Gamma(\psi\to\iota\gamma)}\frac{p_\iota{}^3}{p_{\eta'}{}^3}\right]^{1/2}\left[\frac{m_\iota}{m_{\eta'}}\right]^2=\frac{A_{\eta'}}{A_\iota}\ . \tag{24a}$$

The first ratio is quite well determined, with[21]

$$R^{\rm expt}_{\eta'/\eta}=0.8\pm0.1\ . \tag{23b}$$

The second is only known through the product of branching ratios:[1]

$$B(\psi\to\iota\gamma)B(\iota\to K\bar{K}\pi)\simeq(4.2\pm1.2)10^{-3}\ .$$

If we take the branching ratio for $\iota\to K\bar{K}\pi$ to lie between 30 and 100% we obtain a probably realistic range:

$$R^{\rm expt}_{\eta'/\iota}\simeq\begin{matrix}1.68\pm0.36 & 100\%\ ,\\ 0.92\pm0.20 & 30\%\ .\end{matrix} \tag{24b}$$

All experiments so far performed point to a large $B(\iota\to K\bar{K}\pi)$ so we have concentrated mainly on solutions in that region; but smaller ratios down to 20 or 30% are not yet safely excluded by experiments although the failure so far to see any other channels would be something of a mystery if $B(\iota\to K\bar{K}\pi)$ does turn out to be so small. For comparison however we also discuss solutions with small $K\bar{K}\pi$ branching ratios in the results Sec. IX where we show that the distinction between the two regimes amounts to either suppressed or unsuppressed iota singlet coupling.

(2) PCAC (partial conservation of axial-vector coupling) estimates using the electromagnetic triangle anomaly for two-photon decay. These begin with the PCAC relation between the interpolating *physical* fields $\Phi_a$ for the pseudoscalars $\Pi_a(=\eta,\eta',\iota)$ and the axial divergences via the mixing matrix $F$ of axial decay constants:

$$\partial^\mu A^i_\mu=\sum_a m_a{}^2F_{ia}\Phi_a,\quad i=8,0\ . \tag{25}$$

Since the anomaly gives the amplitude (at $q^2=0$) for the current divergence to two-photon transition, it only requires the solution of (25) for the fields to obtain an estimate of the $\Pi_a\to2\gamma$ transition; but this is only possible in the absence of the $\iota$:

$$r_a\equiv\left[\frac{64\pi^3}{m_a{}^3\alpha_{em}{}^2}\Gamma(\Pi_a\to2\gamma)\right]^{1/2} \tag{26a}$$

$$\simeq\sum_i a_i(F^{-1})A_{ai}\ , \tag{26b}$$

where $a_8=1/\sqrt{3}$, $a_0=2\sqrt{2}/\sqrt{3}$ are the color and flavor factors in the fermion triangle diagram for the anomaly. This inversion is clearly only possible when $F$ is a square nonsingular matrix which applies when the iota is neglected; but in our case $F$ is not a square matrix and has no inverse: the *two* Eqs. (25) for $i=0,8$ cannot be uniquely solved for the *three* interpolating fields. Instead the same considerations involving the triangle anomaly lead to two sum rules:

$$\sum_{a=\eta,\eta',\iota}F_{ia}r_a\approx a_i,\quad i=8,0\ , \tag{27}$$

where (26a) serves as a definition of the $r_a$; two are known from experiment[21] provided these decay amplitudes are slowly varying between $q^2=0$ and $q^2=m_a{}^2$ (we choose $r_\eta$ positive *by convention*—see the Appendix):

$$\begin{aligned}&r_\eta^{\rm exp}=0.78\pm0.06F_\pi{}^{-1}\ \text{ for }\Gamma_\eta=0.32\pm0.05\ \text{keV}\ ,\\ &|r_{\eta'}^{\rm expt}|=1.37\pm0.26F_\pi{}^{-1}\ \text{ for }\Gamma_{\eta'}=5.3\pm1.6\ \text{keV}\ .\end{aligned} \tag{28}$$

The iota decay is of course not yet measured, but theoretical estimates[12–14] span the range 0–20 keV corresponding to $r_\iota\sim0$ to $1.5F_\pi{}^{-1}$; experimental upper limits are around 10 keV (Ref. 21), implying $r_\iota<1F_\pi{}^{-1}$. We certainly have some reservations about taking such estimates too literally since large extrapolations from $q^2=0$ to $m_a{}^2$ are involved in (26) and (27); nevertheless these do provide useful criteria for limiting the range of parameters. However it should be emphasized that our method of solving the WI's in Sec. VI is specifically designed to separate out this part of the analysis so that some results, such as the important topological susceptibility $\chi_t$ are independent of this potential weak link.

(3) Positivity of the spectral functions $\langle\partial^\mu A^i_\mu\partial^\nu A^i_\nu\rangle$ and $\chi_t$: the former is automatically achieved by solving the Ward identities (5); but the latter is obtained from (18) as an *output*, and as we saw in Sec. IV positivity is not automatic and provides a strong restriction on the parameters $F_{0\iota}$ and $A_\iota$ of the heavy iota. This is a crucial assumption.

(4) Finally there are expectations based on the symmetries of QCD: from color SU($N=3$) and the $1/N$ expansion it is likely that glueball couplings $F_{0g}(=F_{0\iota}?)$ are suppressed by $1/\sqrt{N}$ relative to $\bar{q}q$ meson couplings because the glueball only couples to the currents via quark loops. A suppressed coupling as low as $F_{0\iota}\sim\frac{1}{2}F_\pi$ would be consistent with a glueball $\iota$, but is also characteristic of a $\bar{q}q$ radial excitation and therefore not an unambiguous signal for a glueball; an unsuppressed coupling $F_{0\iota}\sim F_\pi$ would probably indicate an ordinary $\bar{q}q$ meson. These are criteria for *interpreting* our final output solutions; but as *input* we make use of the well-known experimental success of flavor-SU(3) symmetry to demand that pseudoscalar $\eta$

and $\eta'$ couplings be "nearly" SU(3) symmetric in the sense discussed in the Introduction. Finally, we assume all amplitudes and couplings which are nonzero in the SU(3) limit have the same sign as $r_\eta$; other choices either violate SU(3) symmetry too much[5] or give numerically the same solutions with different signs. This is not entirely a question of sign conventions, but may at least to some extent, be subjected to experimental test. A discussion appears in the Appendix.

## VI. SOLVING THE ANOMALOUS WARD IDENTITIES

Our procedure for solving the saturated Ward identities is to take five parameters as input: these are $A_{\eta'}/A_\eta=0.8$, which is usually not varied, the parameter $X_{0T}$ defined in Eq. (34), which measures the overall strength of the singlet axial couplings to $\eta$ and $\eta'$; and the iota couplings $F_{8\iota}$, $F_{0\iota}$, and $A_\iota$. For each choice we then obtain a unique solution of the four Eqs. (5). The solution is only accepted if SU(3) violation in the $\eta$ and $\eta'$ axial couplings is smaller than 20% and the output widths for $\eta(\eta')\to 2\gamma$ are broadly acceptable.

The simplest method for solving the Ward identities is first to follow an extension of the technique used in Ref. 5 where the Ward identities (5) are written in an invariant form in the physical three-dimensional $\eta$-$\eta'$-$\iota$ space:

$$\mathbf{X}_8^2=1\ , \tag{29a}$$

$$\mathbf{X}_8\cdot\mathbf{X}_0=\alpha\ , \tag{29b}$$

$$\mathbf{X}_0^2-\mathbf{X}_0\cdot\mathbf{Y}=1\ , \tag{29c}$$

$$\mathbf{X}_8\cdot\mathbf{Y}=0\ . \tag{29d}$$

The three-dimensional vectors have components defined by

$$X_{8a}\equiv\alpha_8 m_a F_{8a}\ , \tag{30a}$$

$$X_{0a}\equiv\alpha_0 m_a F_{0a}\ , \tag{30b}$$

$$Y_a\equiv\alpha_0 m_a A_a\ , \tag{30c}$$

for $a=\eta,\eta',\iota$, where

$$\alpha_8\equiv[\tfrac{1}{3}(4m_k{}^2F_K{}^2-m_\pi{}^2F_\pi{}^2)]^{-1/2}$$
$$=0.22\pm0.02(m_\pi F_\pi)^{-1}\ , \tag{31a}$$

$$\alpha_0\equiv[\tfrac{1}{3}(2m_K{}^2F_K{}^2+m_\pi{}^2F_\pi{}^2)]^{-1/2}$$
$$=0.31\pm0.03(m_\pi F_\pi)^{-1}\ , \tag{31b}$$

and

$$\alpha\equiv-\frac{2\sqrt{2}}{3}(m_K{}^2F_K{}^2-m_\pi{}^2F_\pi{}^2)\alpha_0\alpha_8=-0.93\pm0.08 \tag{31c}$$

with $F_K=(1.1\pm0.5)F_\pi$ and $F_\pi=(93.0\pm0.2)$ MeV. The crucial step now is to observe that the Ward identities (29) are invariant under rotations in the $\eta$-$\eta'$-$\iota$ plane. This requires extra input to find the physical components (30), but has the advantage that (29) may be solved in any convenient coordinate system; the extra physical input is needed only subsequently to identify the physical axes. Since the iota couplings are being taken as input, the third component and the iota axes are assumed known and fixed: the only ambiguity remaining is rotations in the $\eta$-$\eta'$ plane about the iota axis. Suppose there is a convenient set of axes $x$-$y$ in the $\eta$-$\eta'$ plane where it is simple to solve the Ward identities (29). It then only requires one additional physical input, such as $R_{\eta'/\eta}$, to find the matrix $\Omega(\phi)$ which rotates the $x$-$y$ axes by angle $\phi$ to the physical axes and hence to obtain the physical couplings and topological charges by the same rotation of the vectors.

The most convenient set of axes [Fig. 2(a)] is one where $z=\iota$ and the unit vector $\mathbf{X}_8$ lies in the $x$-$\iota$ plane; (29a) immediately gives this vector uniquely modulo a single unknown sign which we choose positive:

$$\mathbf{X}_8=\begin{pmatrix}(1-X_{8\iota}{}^2)^{1/2}\\0\\X_{8\iota}\end{pmatrix}\ . \tag{32a}$$

The remaining equations are then immediately solved in terms of a single unknown constant $X_{0T}$ and modulo a second arbitrary sign which is again chosen positive:

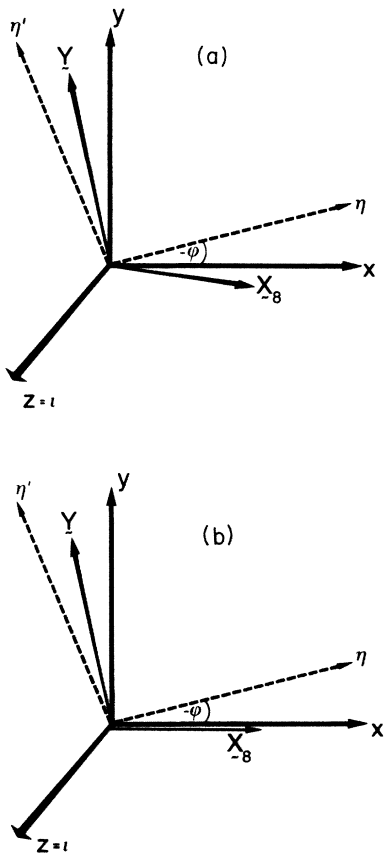


FIG. 2. (a) Coordinate systems in $\eta$-$\eta'$-$\iota$ space. (b) Coordinate systems in $\eta$-$\eta'$-$\iota$ space in the absence of mixing with the iota.

$$\mathbf{X}_0=\begin{bmatrix} a \\ (X_{0T}{}^2-a^2)^{1/2} \\ X_{0\iota} \end{bmatrix} \tag{32b}$$

and

$$\mathbf{Y}=\begin{bmatrix} -bX_{8\iota}Y_\iota \\ \dfrac{[X_0{}^2-1-Y_\iota(X_{0\iota}-X_{8\iota}ab)]}{(X_{0T}{}^2-a^2)^{1/2}} \\ Y_\iota \end{bmatrix}, \tag{32c}$$

where

$$a\equiv b(\alpha-X_{0\iota}X_{8\iota}) \tag{33a}$$

and

$$b\equiv(1-X_{8\iota}{}^2)^{-1/2}\,. \tag{33b}$$

The parameter $X_{0T}$ represents the length of the projection of $\mathbf{X}_0$ onto the $\eta$-$\eta'$ plane and is still unknown; given $X_{0\iota}$ its value fixes the length of $\mathbf{X}_0$:

$$X_0{}^2=X_{0T}{}^2+X_{0\iota}{}^2\,. \tag{34}$$

This plays the role previously taken by $X_0$ when the iota was neglected[5] and $a$ role taken by $\alpha$ [see Fig. 2(b)]:

$$\mathbf{X}_8=\begin{bmatrix}1\\0\end{bmatrix},\quad \mathbf{X}_0=\begin{bmatrix}\alpha\\(X_0{}^2-\alpha^2)^{1/2}\end{bmatrix},\quad \mathbf{Y}=\begin{bmatrix}0\\\dfrac{(X_0{}^2-1)}{(X_0{}^2-\alpha^2)^{1/2}}\end{bmatrix}. \tag{35}$$

It will be shown subsequently that the parameter $X_{0T}$ is essentially fixed by the $2\gamma$ decays and approximate SU(3) symmetry to be around $2(m_\pi F_\pi)^{-1}$.

The question of the two undetermined signs together with the unknown signs of relevant decay amplitudes is discussed in the Appendix where we show how they feature in the solutions: there are only two sets of *numerically* distinct solutions; one is approximately SU(3) symmetric and is the one chosen here; the other violates SU(3) badly. We also show how, at least in principle, experiments can distinguish between some of the different choices that still remain.

Finally we come to the rotation $\Omega(\phi)$ to the physical $\eta$-$\eta'$-$\iota$ axes which is given in terms of the $\psi$-decay parameter defined in Eqs. (23):

$$\tan\phi=\frac{rY_x-Y_y}{Y_x+rY_y}\,, \tag{36a}$$

where

$$r=\frac{m_{\eta'}A_{\eta'}}{m_\eta A_\eta}=\frac{m_{\eta'}}{m_\eta}R_{\eta'/\eta}\,. \tag{36b}$$

In the absence of the iota, or when it does not mix into the octet ($F_{8\iota}=0$) we regain the simple result[5]

$$\tan\phi=-\frac{1}{r} \tag{36c}$$

which is the appropriate condition accompanying Eq. (35). In both cases the rotation matrix is

$$\Omega(\phi)=\begin{bmatrix}\cos\phi&-\sin\phi&0\\\sin\phi&\cos\phi&0\\0&0&1\end{bmatrix}, \tag{37}$$

where the rows and columns are labeled in the order $\eta,\eta',\iota$ and $x,y,\iota$, respectively (see Fig. 2).

Thus, for each choice of $X_{0T}$ and of the iota couplings $F_{8\iota},F_{0\iota},A_\iota$ there is a unique set of vectors given by the Eqs. (32). Imposition of the conditions (36) related to $\psi\to\eta(\eta')\gamma$ decays then fixes the rotation $\Omega(\phi)$ to physical $(\eta\eta'\iota)$ axes. Next the criteria discussed in Sec. V are used to fix or at least narrow down the range of the four so far arbitrarily chosen parameters: the "measured" decay $\psi\to\iota\gamma$, Eqs. (24a) and (24b); positivity of the topological susceptibility which, as we noted in Sec. II constrains the size of $(F_{0\iota}-A_\iota)$ and, as we shall see shortly, provides a particularly powerful restriction on $A_\iota$; and finally, near SU(3) symmetry. We now proceed to discuss our solutions, starting from the general case and imposing in turn each set of restrictions from the most powerful down to the least, finally ending up with a restricted range of parameters which are used to delimit the expected width for $\iota\to2\gamma$. We begin with the most important constraint: positivity of topological susceptibility.

## VII. TOPOLOGICAL SUSCEPTIBILITY EVALUATED

The topological susceptibility defined by Eq. (6) is obviously flavor independent and therefore invariant under rotations in the $\eta$-$\eta'$-$\iota$ plane; consequently it is independent of the rotation angle $\phi$ and may be computed from the solution (32) of the Ward identities without any further input. Using the WI (17), its saturation (18), and the definitions (30) we obtain

$$6\chi_t=\frac{1}{\alpha_0{}^2}(\mathbf{X}_0\cdot\mathbf{Y}-\mathbf{Y}^2) \tag{38a}$$

$$=\frac{1}{\alpha_0{}^2}(\mathbf{X}_0{}^2-1-\mathbf{Y}^2)\,, \tag{38b}$$

where the last line follows from the WI (29c). This is a quadratic form in $Y_\iota$ which is plotted in Fig. 3. A compact expression may be written in terms of the two variables

$$y_\iota=Y_\iota-X_{0\iota}+\alpha X_{8\iota}\,,$$

$$x_{0\iota}=(X_{0\iota}-\alpha X_{8\iota})/(1-X_{8\iota}{}^2)\,,$$

and the small quantity of order $(m_\pi/m_K)^2$:

$$\delta\equiv1-\alpha^2$$

$$=\frac{9(m_\pi F_\pi)^2(2m_K{}^2F_K{}^2-m_\pi{}^2F_\pi{}^2)}{(4m_K{}^2F_K{}^2-m_\pi{}^2F_\pi{}^2)(2m_K{}^2F_K{}^2+m_\pi{}^2F_\pi{}^2)}\approx0.13\,, \tag{39}$$

$$6\chi_t=\frac{[(X_0{}^2-x_{0\iota}{}^2-1)\delta-2y_\iota x_{0\iota}\delta-y_\iota{}^2(X_0{}^2-\alpha^2)]}{\alpha_0{}^2(X_0{}^2-x_{0\iota}{}^2-\alpha^2)}\,. \tag{40}$$

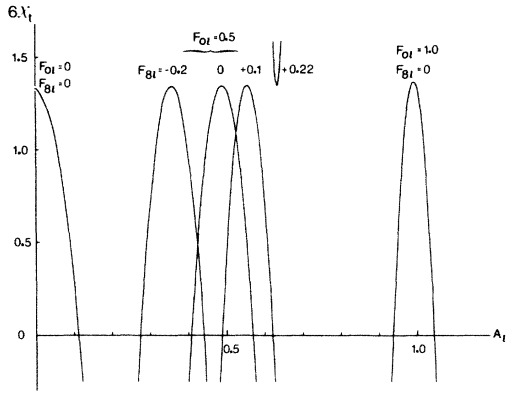


FIG. 3. Regions of positive topological susceptibility for $X_{0T}=1.9$. The units in this and all subsequent figures use $m_\pi=1$, $F_\pi=1$.

The small value of $\delta$ is responsible for the narrow range of $y_\iota$—or of $(F_{0\iota}-A_\iota)$—for which $\chi_t$ is positive. With the exception of the region $F_{8\iota}\geq+0.2$ [which is excluded by approximate SU(3) symmetry, see Fig. 9, and $\eta'\to2\gamma$, see Fig. 18] we find the permitted range for the topological susceptibility:

$$0\leq 6\chi_t\leq 1.36(m_\pi F_\pi)^2 \tag{41}$$

or

$$0\leq\chi_t\leq(79\text{ MeV})^4 .$$

Figure 4 summarizes this tight correlation between $F_{0\iota}$ and $A_\iota$ for our favored choice of octet coupling, $F_{8\iota}=-0.2$; Fig. 5 shows that approximate SU(3) symmetry favors the region $\chi_t\approx0$ corresponding to the largest allowed value for $A_\iota$. A further interesting property of the topological susceptibility is evident in Fig. 3: the maximum point is independent of the octet couplings. It

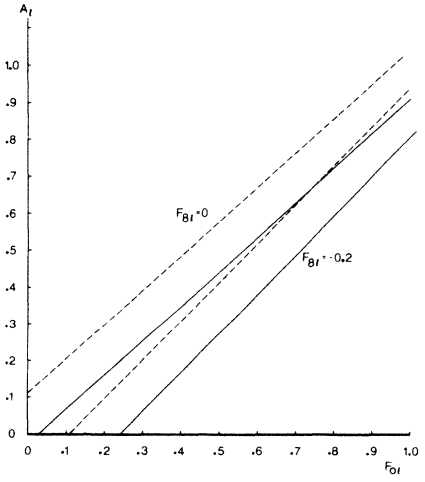


FIG. 4. Allowed ranges of $F_{0\iota}$ and $A_\iota$ corresponding to positive susceptibility lie in the narrow region between pairs of lines. Two values of $F_{0\iota}$ are shown for the choice $X_{0T}=1.9$.

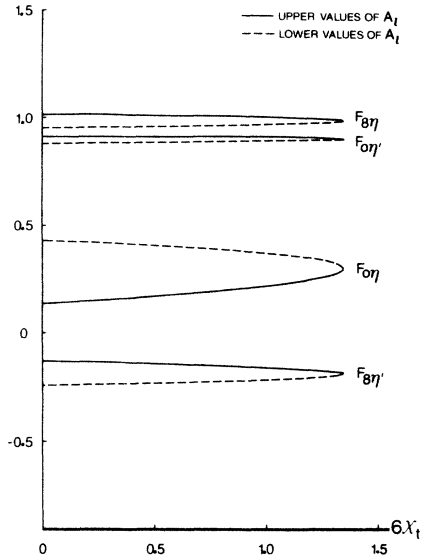


FIG. 5. Variation of axial-vector couplings with topological susceptibility for $X_{0T}=1.9$, $F_{0\iota}=0.5$, $F_{8\iota}=-0.2$. The solid and dashed curves correspond to the two values of $A_\iota$ obtained from the appropriate curve in Fig. 3.

is also virtually independent of all the other $\eta$, $\eta'$, and $\iota$ couplings—again a consequence of the small size of $\delta$:

$$6\chi_t^{\max}=\frac{\delta}{\alpha_0^2}\frac{(X_0^2-1)}{(X_0^2-\alpha^2)} \tag{42a}$$

$$=\frac{\delta}{\alpha_0^2}\left[1-\frac{\delta}{(X_0^2-\alpha^2)}\right] \tag{42b}$$

$$\approx\tfrac{3}{2}(m_\pi F_\pi)^2\left[\frac{2m_K^2F_K^2-m_\pi^2F_\pi^2}{2m_K^2F_K^2-m_\pi^2F_\pi^2}\right] \tag{42c}$$

$$=1.38(m_\pi F_\pi)^2 . \tag{42d}$$

To obtain the approximation (42c) we discarded the second term in the large parentheses of (42b) which is typically of order 5%. This is the case because the physically interesting region corresponds to:

$$\mathbf{X}_0^2\geq X_{0\eta'}^2=m_{\eta'}^2\alpha_0^2F_{0\eta'}^2\approx m_{\eta'}^2\alpha_0^2F_\pi^2\approx\frac{3}{2}\left[\frac{m_{\eta'}}{m_K}\right]^2\approx5.6$$

which makes the denominator in the correction term safely large.

Thus, not only do we conclude that $\chi_t$ is small, but that it is largely independent of the uncertain properties of the pseudoscalars. This is not the case for the "subtraction" $\chi_t^0$, although it is still independent of the flavor rotation angle $\phi$. From Eq. (19b),

$$6\chi_t^0=\frac{(X_0^2-1)}{\alpha_0^2} . \tag{43}$$

This is plotted in Fig. 6 with the iota coupling dependence

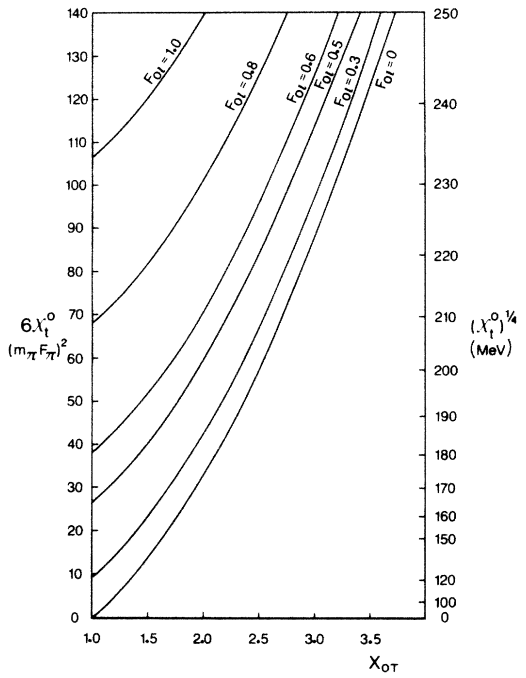


FIG. 6. The subtraction topological susceptibility $\chi_t^0(\sim\chi_t^{YM})$ according to Eq. (44).

made explicit. Comparison with Eq. (42a) leads to the relation

$$6\chi_t^0=\frac{(X_0^2-\alpha^2)}{\delta}6\chi_t^{\max} \tag{44}$$

which shows clearly the large enhancement effect of order 30.

To summarize, positivity of $\chi_t$ restricts both the range of $(F_{0\iota}-A_\iota)$ [Eq. (42) and Fig. 4] and of $\chi_t$ itself [Eq. (41) and Fig. 3]. Since the topological susceptibility is flavor independent and has such a restricted range of variation it is most convenient to choose $\chi_t$ as an *input* parameter; approximate SU(3) symmetry favors $\chi_t\approx 0$, corresponding to the largest permissible value for $A_\iota$ [Fig. 5 and Eq. (40)]. Thus given $\chi_t$, $X_{0T}$, $F_{0\iota}$, and $F_{8\iota}$ we may obtain the topological charge $A_\iota$ by solving Eq. (40). *These are taken as our input parameters.*

## VIII. A SIMPLE CASE: NO OCTET MIXING IN THE IOTA

Before proceeding to a more detailed analysis based on the restrictions discovered in the previous section, it is useful first to study a simplified model system where the iota is a pure SU(3) singlet. To avoid any confusion with previous and subsequent sections and to emphasize that this section may serve as a paradigm for the unmixed glueball we denote the iota as $g$: this stands for the approximation $F_{8\iota}=0$.

With $F_{8\iota}\equiv F_{8g}=0$ the solutions are as depicted in Fig. 2(b), with the simple form obtained directly from Eqs. (32):

$$\mathbf{X}_8=\begin{bmatrix}1\\0\\0\end{bmatrix}, \tag{45a}$$

$$\mathbf{X}_0=\begin{bmatrix}\alpha\\(X_{0T}^2-\alpha^2)^{1/2}\\X_{0g}\end{bmatrix}, \tag{45b}$$

$$\mathbf{Y}=\begin{bmatrix}0\\\dfrac{X_{0T}^2-1-X_{0g}y_g}{X_{0T}^2-\alpha^2}\\Y_g\end{bmatrix}. \tag{45c}$$

Note the similarity to the iota-less solution (35): $X_{0T}$ plays the role of $X_0$, and there is a correction term in the second component of (45c) which is small because positivity of topological charge requires $y_g$ to be small. Moreover, the rotation angle $\phi$ is now given by (36c) rather than the more complicated (36a).

The topological susceptibility is now greatly simplified and may be cast into the form

$$6\chi_t\simeq\frac{1}{\alpha_0^2(X_{0T}^2-\alpha^2)}[(X_{0T}^2-1)\delta-2X_{0g}y_g\delta -(X_0^2-\alpha^2)y_g^2] \tag{46}$$

which is positive in the range between the two roots:

$$A_g\approx F_{0g}\left[1-\frac{\delta}{(X_0^2-\alpha^2)}\right]\pm\frac{1}{\alpha_0 m_g}\left[\frac{(X_{0T}^2-1)}{(X_0^2-\alpha^2)}\delta\right]^{1/2}, \tag{47}$$

where a term of $O(\delta^2)$ has been dropped in the square root. This shows clearly the role of the small quantity $\delta$ defined in Eq. (39) in restricting the range of $(A_g-F_{0g})$.

## IX. RESULTS

The procedure we adopt for obtaining numerical solutions starts with a choice of five input parameters: these are $A_{\eta'}/A_\eta=0.8$ as given by Eq. (23); the parameter $X_{0T}$ measuring the overall singlet coupling strength of $\eta$ and $\eta'$; the topological susceptibility $6\chi_t$ which only spans a narrow possible range given in Eq. (41); and finally, the two iota couplings $F_{0\iota}$,$F_{8\iota}$, Equation (40), depicted in Fig. 3, then immediately gives two values for the third iota coupling $A_\iota$ and Eqs. (32) provide solutions to the Ward identities (29), although at this stage only in the special $x$-$y$-$\iota$ coordinate system. The information on the ratio $A_{\eta'}/A_\eta$ obtained from the $\psi$ radiative decays is now used to rotate the coupling vectors to the physical $\eta$-$\eta'$-$\iota$ axes via Eqs. (36) and (37). This completes the solution which is now subjected to three tests.

*Test (1).* Deviations from SU(3) symmetry are minimized. This is most important in fixing a value for $X_{0T}$ as shown in Fig. 7: $F_{0\eta}$ and $F_{0\eta'}$ are not only strongly dependent on $X_{0T}$ but serve to bracket the region around $X_{0T}\simeq 1.9\pm 0.1$ rather convincingly. In passing we note

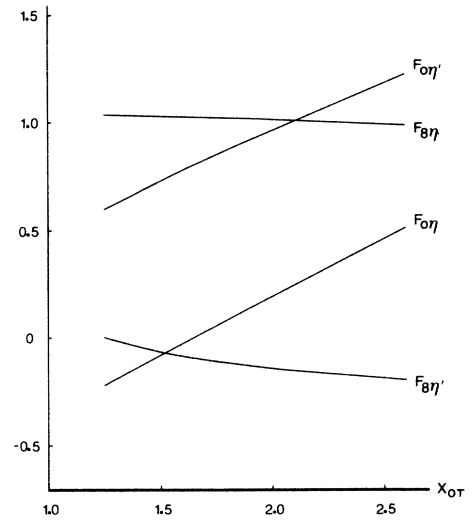


FIG. 7. Variation of axial-vector couplings with $X_{0T}$ for $F_{0\iota}=0.5$, $F_{8\iota}=-0.2$, and $\chi_t=0$ (the latter corresponding to the choice $A_\iota=0.44$).

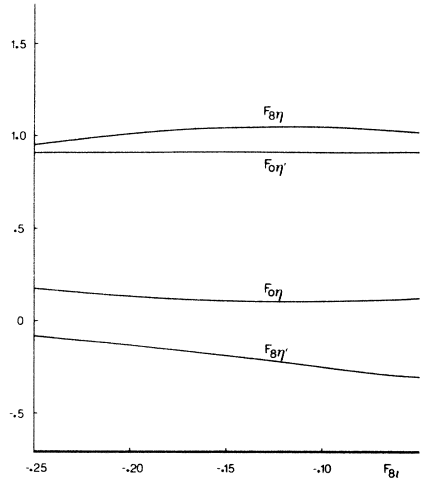


FIG. 9. Variation of axial-vector couplings with $F_{8\iota}$ for $F_{0\iota}=0.5$, $\chi_t=0$ (with the choice $A_\iota=0.44$) and $X_{0T}=1.9$.

that although Fig. 7 corresponds to fixed values for all the other four input parameters we have of course checked by a thorough search that the trends are the same for other values. This general comment applies to all the figures presented in this paper. $F_{8\eta}$ and $F_{8\eta'}$ are only weakly dependent on $X_{0T}$ in the viable range of iota couplings for the following reason: Eq. (32a) implies that they only depend on $X_{0T}$ through the rotation angle $\phi$; but Eqs. (36) imply that the latter is only dependent on $X_{0T}$ when $F_{8\iota}\neq 0$; since $F_{8\iota}$ turns out to be small $\phi$ is therefore only weakly dependent on $X_{0T}$.

Figure 8 shows that the SU(3)-symmetry test also provides some constraints on $F_{0\iota}$ from the behavior of $F_{0\eta}$ and $F_{8\eta'}$:

$$0.4<F_{0\iota}<0.8\ . \tag{48a}$$

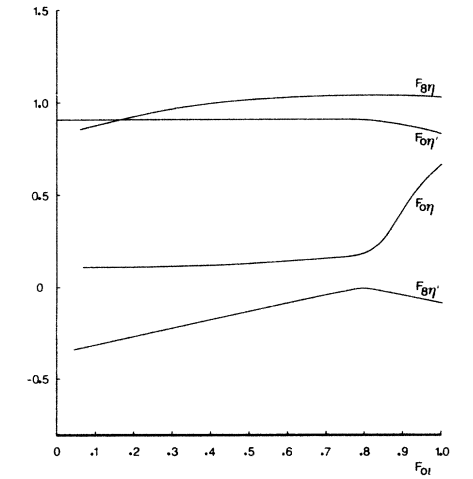


FIG. 8. Variation of axial-vector couplings with $F_{0\iota}$ for $F_{8\iota}=-0.2$, $\chi_t=0$ (with the choice $A_\iota=0.44$) and $X_{0T}=1.9$.

A similar type of constraint is imposed on $F_{0\iota}$ by the behavior of the same two couplings shown in Fig. 9:

$$-0.25<F_{8\iota}<-0.15\ . \tag{49}$$

The reason why $F_{8\iota}$ comes out negative is closely related to the reason for the negative sign of $F_{8\eta}$ (Ref. 5). The relevant WI is Eq. (5d) which gives

$$F_{8\eta'}=-\left[\frac{m_\eta}{m_{\eta'}}\right]^2\frac{A_\eta}{A_{\eta'}}F_{8\eta}-\left[\frac{m_\iota}{m_{\iota'}}\right]^2\frac{A_\iota}{A_{\eta'}}F_{8\iota}\ . \tag{50}$$

We have chosen the signs of $A_\eta/A_{\eta'}$, $A_\iota/A_{\eta'}$, and $F_{8\eta}$ positive; therefore in the absence of the iota contribution $F_{8\eta'}$ is negative. If $F_{8\iota}$ were positive the iota term would then enhance the $\eta$ contribution thereby increasing the magnitude of $F_{8\eta'}$ and the accompanying SU(3) breaking. It is not possible to alter the first term in (50) to compensate for this effect because $F_{8\eta}$ is also constrained by SU(3) symmetry and the other factors in the first term are fixed. Thus negative values of $F_{8\iota}$ are favored; moreover its magnitude cannot be very large because the sign-independent WI (5a) for the octet couplings is already nearly saturated by the $\eta$ contribution, which itself cannot be reduced too much without large SU(3) breaking.

*Test (2).* A further confirmation of the SU(3) restrictions on $F_{0\iota}$ and $F_{8\iota}$ comes from the $\psi\to\iota\gamma$ decay. It seems most likely that the $\iota\to K\bar{K}\pi$ channel is overwhelmingly the dominant one, so that we first choose to bias our discussion toward the larger value of $R_{\eta'/\eta}$ in Eqs. (24). Figures 10 and 11 show that a satisfactory fit to this data is obtained for a range of $F_{0\iota}$ and $F_{8\iota}$ compatible with that singled out by SU(3) symmetry with Fig. 10 suggesting a slightly tighter restriction on $F_{0\iota}$:

$$F_{0\iota}\simeq(0.5\pm 0.1)F_\pi\ . \tag{48b}$$

Our success in being able to obtain such a large ratio $R_{\eta'/\iota}$ stems from the positivity constraint on $\chi_t$: a suppressed

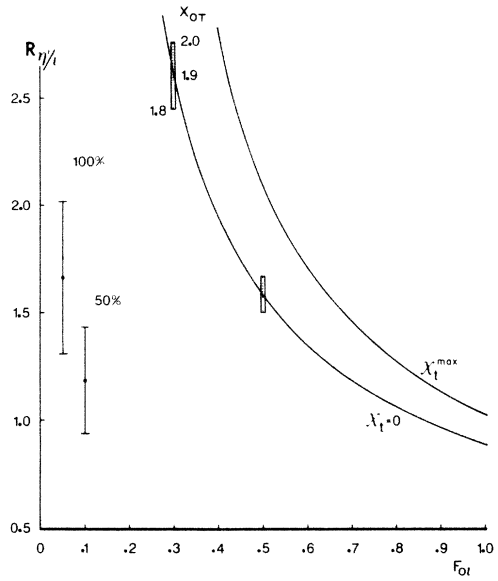


FIG. 10. Variation of $R_{\eta'/\iota}$ [defined by Eq. (24a)] with $F_{0\iota}$ for $F_{8\iota}=-0.2$, $X_{0T}=1.9=-0.1$, and two values of the topological susceptibility. For $\chi_t=0$ the value if $A_\iota$ chosen is the largest, corresponding to the least SU(3) breaking (see Fig. 5); for $\chi_t^{max}$ there is a unique value for $A_\iota$.

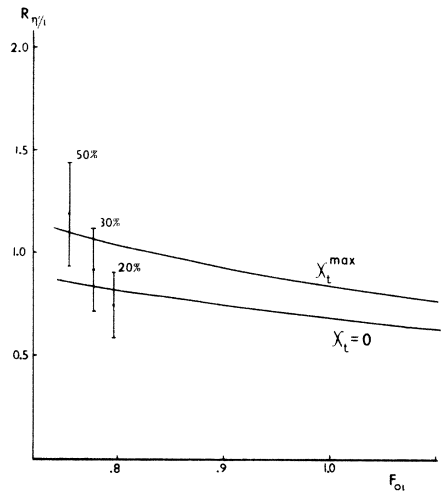


FIG. 12. Same as Fig. 10, but with $F_{8\iota}=-0.10$ corresponding to small branching ratios for $\iota\to K\bar{K}\pi$.

$F_{0\iota}\simeq 0.5F_\pi$ leads via positivity to a suppressed $A_\iota\approx F_{0\iota}$ [Eq. (47)] and hence an enhanced $R_{\eta'/\iota}$ Eq. (24a)]. The current experimental position is that only the $\iota\to K\bar{K}\pi$ channel has so far been seen;[1,2] but these are difficult experiments and there are also theoretical arguments[2] which suggest that this may not be the dominant channel. We therefore consider it useful to contrast the above analysis with one where we take $B(\iota\to K\bar{K}\pi)$ to lie as low as 20—30%. According to Eq. (24a) this requires an increase in $A_\iota$ and therefore [Eq. (47)] in $F_{0\iota}$; but we have already noted in Fig. 8 that values of $F_{0\iota}>0.8$ lead to unacceptable symmetry breaking in $F_{0\eta}$, and so this should be considered an upper limit. Figures 12 and 13 show that there is no difficulty in obtaining 20—30% branching ratios albeit with somewhat greater symmetry breaking in $F_{0\eta}$ because larger values of $F_{0\iota}$ are required.

*Test (3).* A tighter limitation on the acceptable range of $F_{0\iota}$ and $F_{8\iota}$ requires a use of the more problematic $2\gamma$ decay constraints. This is why we chose to solve the WI's without imposing the two sum rules (27) at the beginning. One difficulty stems from the fact that the PCAC predictions are derived for the off-mass-shell point $q^2=0$—giving a "width" $\Gamma^{theor}\equiv\Gamma(0)$ which needs to be extrapolated to the quite distant mass shell point $q^2=m_a{}^2$ to provide a comparison with the measurements, $\Gamma^{expt}=\Gamma(m_a{}^2)$. In studying the sum rules (27) we chose to view the least

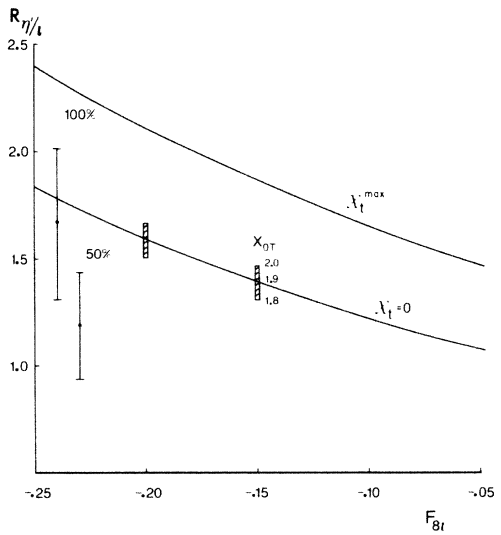


FIG. 11. Variation of $R_{\eta'/\iota}$ with $F_{8\iota}$ for $F_{0\iota}=0.5$, $X_{0T}=1.9\pm0.1$. See Fig. 10 for further explanations.

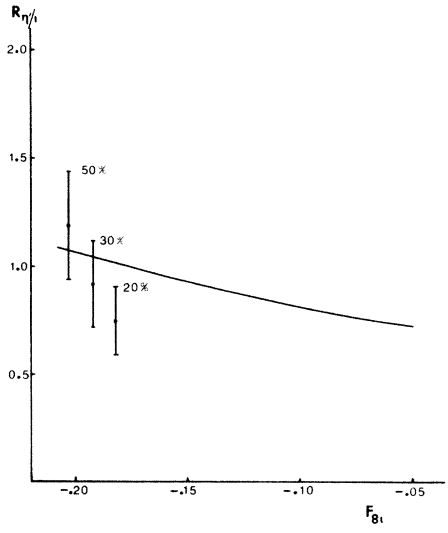


FIG. 13. Same as Fig. 11 but with $F_{0\iota}=0.8$ corresponding to small branching ratios for $\iota\to K\bar{K}\pi$.

problematic $\eta$ width as *input* and the $\eta',\iota$ widths as *output,* obtained from solving the two linear Eqs. (27):

$$r_{\eta'}=\frac{(a_8F_{0\iota}-a_0F_{8\iota})-r_\eta(F_{8\eta}F_{0\iota}-F_{0\eta}F_{8\iota})}{D}\ , \tag{51a}$$

$$r_\iota=\frac{(a_0F_{8\eta'}-a_8F_{0\eta'})+r_\eta(F_{8\eta}F_{0\eta'}-F_{0\eta}F_{8\eta'})}{D}\ , \tag{51b}$$

where the determinant is

$$D\equiv F_{8\eta'}F_{0\iota}-F_{0\eta'}F_{8\iota}\ . \tag{51c}$$

We then kept in mind that the corresponding widths $\Gamma^{\text{theor}}$ may change by considerably more than the quoted experimental errors in extrapolating to the mass shell. To estimate the effect an off-mass-shell extrapolation might have, we consider, perhaps somewhat optimistically, a form

$$\Gamma(m_a{}^2)=\Gamma(0)\left[1\pm\left[\frac{m_a}{M}\right]^2\right]\ . \tag{52}$$

Assuming that gluons have something to do with the dynamics of this extrapolation we take a glueball-like mass $M\sim 1.5$ GeV. Figures 14 and 15 show how the extrapolated values are connected with the $q^2=0$ values; when we also take into account of the experimental errors we obtain an "estimate" for the range of output values we consider reasonable:

$$\begin{aligned}&\Gamma_{\eta\to 2\gamma}(0)\sim 0.32^{+0.08}_{-0.06}\ \text{keV}\ ,\\ &\Gamma_{\eta'\to 2\gamma}(0)\sim 5.3^{+4}_{-2}\ \text{keV}\ .\end{aligned} \tag{53}$$

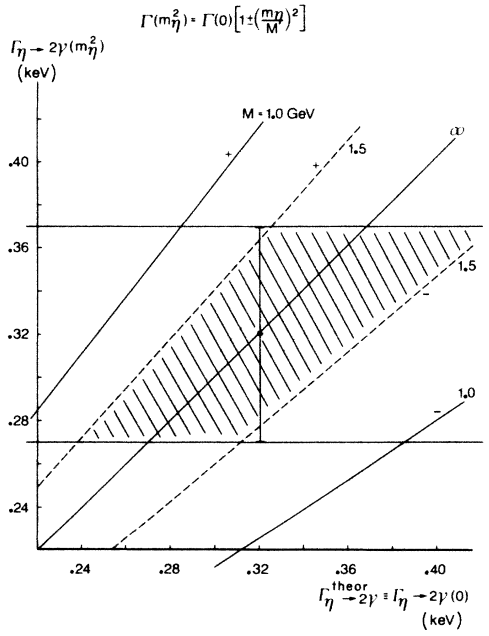


FIG. 14. $\eta\to 2\gamma$ widths at $q^2=0$ versus on-mass-shell values according to the prescription (52). The hatched region given by the "experimental" error bar corresponds to the range of $q^2=0$ values used in the text. The labels ± refer to the sign of the extrapolation term.

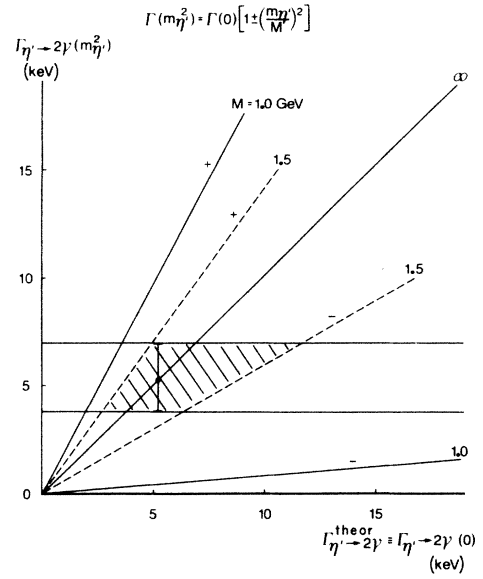


FIG. 15. Same as Fig. 14 but for $\eta'\to 2\gamma$.

This may be too pessimistic; but a recent analysis of the $\pi^0\to 2\gamma$ process by Kitazawa[22] indicates that the extrapolation to the mass shell might in that case amount to as much as 10%. Although undoubtedly the dynamics of the isoscalar $\eta$ and $\eta'$ are different from the $\pi^0$ the extrapolation is from four to seven times further and so we should not be too surprised if we have 40—70% effects. In a similar way the iota extrapolation may be uncertain to something like a factor of 2. There is another more hopeful point of view, however: since we are using the

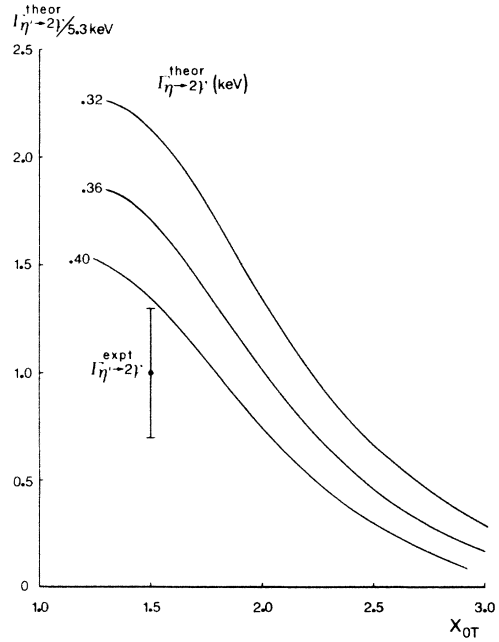


FIG. 16. Variation of $q^2=0$ widths with $X_{0T}$ for $F_{0\iota}=0.5$, $F_{8\iota}=-0.20$ and $\chi_\iota=0$ (corresponding to $A_\iota=0.44$).

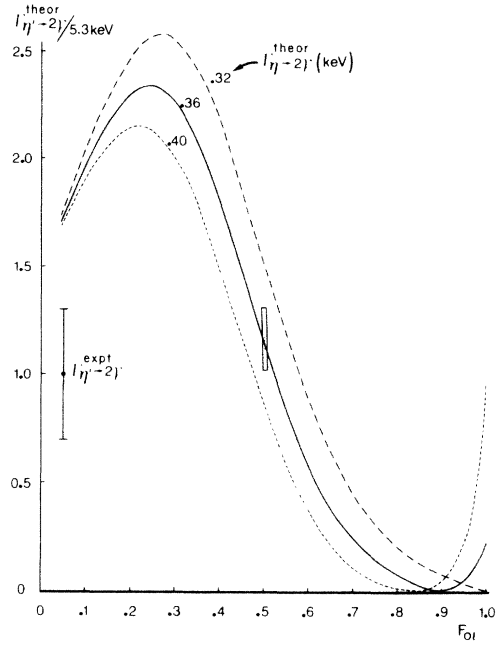


FIG. 17. Variation of $q^2=0$ widths with $F_{0\iota}$ for $F_{8\iota}=-0.20$, $X_{0T}=1.9$ and $\chi_t=0$ (corresponding to $A_\iota=0.44$).

soft-meson theorem as two sum rules (27) and calculating the $\eta'$ and $\iota$ widths in terms of the $\eta$ width, not absolutely, it may be that the sum rules are valid well beyond $q^2=0$.

Keeping these comments very much in mind we now consider solutions corresponding to large $\iota\to K\bar{K}\pi$ branching ratios. Figures 16, 17, and 18 show the output $\eta'$ widths for a range of input $\eta$ widths to illustrate that acceptable values occur in the range of coupling parameters singled out by the previous tests. In general the $\eta'$ widths are very sensitive to the iota couplings and are quite unacceptable outside the ranges illustrated here. The rapid variation in Fig. 17 around $F_{0\iota}\simeq F_\pi$ and particularly in Fig. 16 around $F_{8\iota}\approx -0.12F_\pi$ come from zeros in the denominator $D$. Fortunately the solutions with large $\iota\to K\bar{K}\pi$ branching ratio do not approach this dangerous region too closely, and we conclude that the parameter values singled out by our previous considerations also provide remarkably sensible values for the $\eta$ and $\eta'\to 2\gamma$ widths. Although not apparent in these figures, a thorough computer search has shown that in fact this region is strongly singled out: all other parameter combinations either give very large SU(3)-symmetry breaking, unacceptable values for $R_{\eta'/\iota}$ or lead to $2\gamma$ widths far outside any conceivable extrapolation range. That acceptable values for $\iota\to 2\gamma$ are possible is shown in Fig. 19 where we also see a complicated behavior induced by nearby zeros of both the numerator (at $F_{8\iota}\simeq -0.15$) and denominator (at $F_{8\iota}\simeq -0.10$) in Eq. (51b). This sensitivity is again outside the parameter range of this solution and so should not influence the output iota width too seriously. Figure 20 which plots the *amplitudes* provides a convenient summary and helps to emphasize that small values of the $\iota\to 2\gamma$ width tend to be favored when $F_{0\iota}\simeq(0.5\pm 0.1)F_\pi$ and when the $\eta'\to 2\gamma$ width comes within the acceptable range given in (53). This concludes

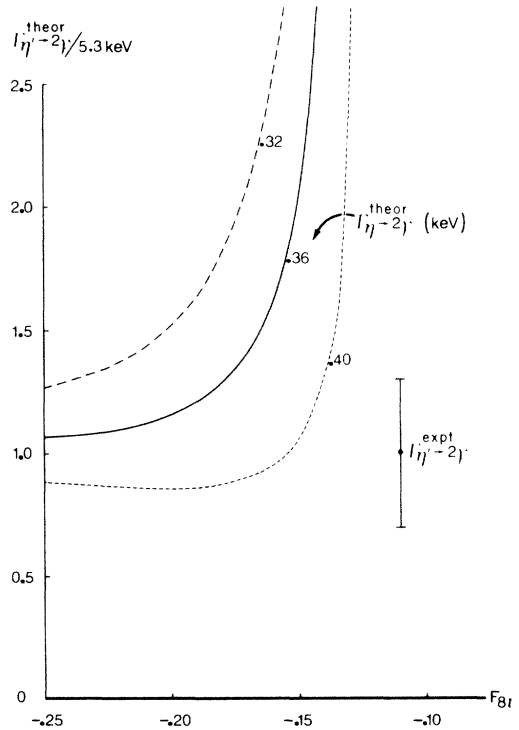


FIG. 18. Variation $q^2=0$ widths with $F_{8\iota}$ for $F_{0\iota}=0.5$, $X_{0T}=1.9$ and $\chi_t=0$ (corresponding to $A_\iota=0.44$).

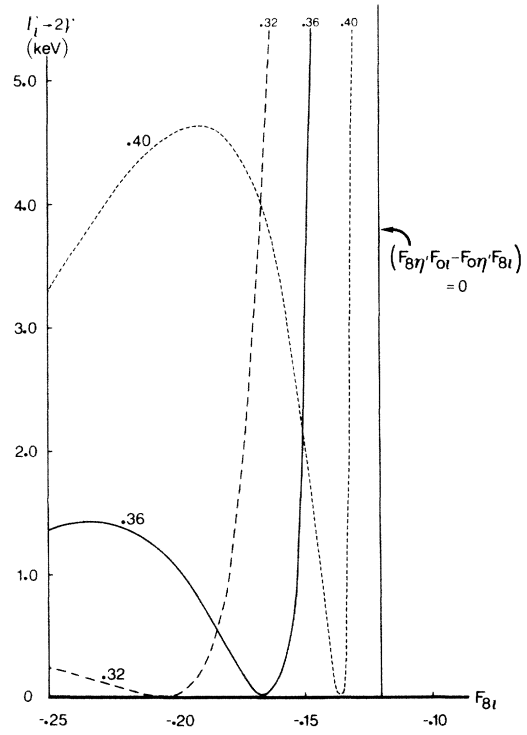


FIG. 19. Variation of iota widths at $q^2=0$ with $F_{8\iota}$ for $F_{0\iota}=0.5$, $X_{0T}=1.9$, and $\chi_t=0$ (corresponding to $A_\iota=0.44$).

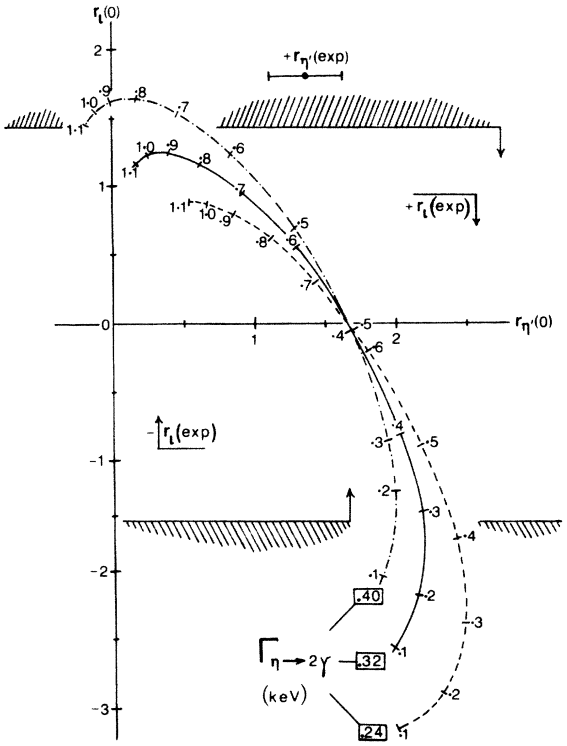


FIG. 20. Correlation between output $2\gamma$ *amplitudes* for $F_{8\iota}=-0.20$, $X_{0T}=1.9$, and $\chi_\iota=0$ (corresponding to $A_\iota=0.44$). The numbers marked on each curve are values of $F_{0\iota}$. Experimental upper limits for the iota width (Ref. 21) indicated by the hatched and plain horizontal lines correspond to the likely range of branching ratios for $\iota\to K\bar{K}\pi$; the lowest to 100%. Note that only positive values of $r_\eta$ are compatible, but either sign of $r_\iota$ is allowed.

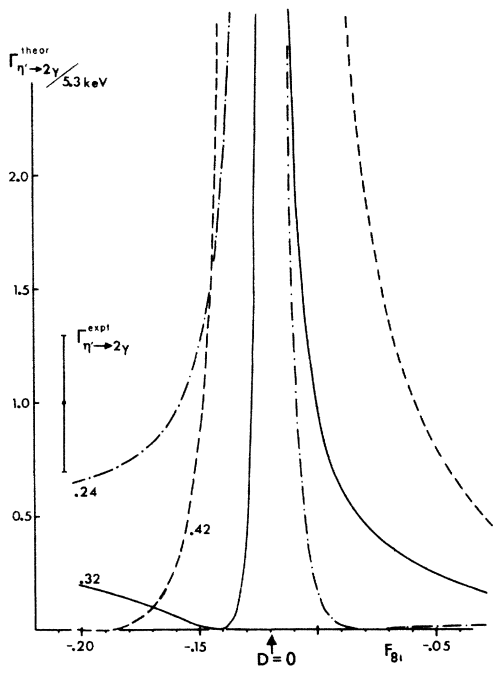


FIG. 21. Variation of $\eta'\to 2\gamma$ output width with $F_{8\iota}$ for solutions possessing small $\iota\to K\bar{K}\pi$ branching ratios (compare Fig. 18); for $F_{0\iota}=0.8$, $X_{0T}=1.9$, and $\chi_\iota=0$ (corresponding to $A_\iota=0.44$). Note the rapid variations caused by nearby zeros in numerator and denominators in Eq. (51).

our presentation of the solution with suppressed singlet coupling $F_{0\iota}$: its main distinguishing feature is a large ratio $F_{\eta'/\iota}$ corresponding to an amplitude for $\psi\to\iota\gamma$ a good deal smaller than one might expect for a glueball. Such a large ratio seems to be favored by the data which points to a nearly 100% branching ratio for $\iota\to K\bar{K}\pi$.

There is one other small window in parameter space where acceptable solutions may occur, and this corresponds to small branching ratios,

$$B(\iota\to K\bar{K}\pi)\simeq 20\% , \tag{54a}$$

and larger singlet couplings:

$$F_{0\iota}\simeq(0.8\text{–}0.9)F_\pi . \tag{54b}$$

This is the region of parameter space considered above and depicted in Figs. 12 and 13. Unfortunately Figs. 21 and 22 together show that to obtain acceptable output $2\gamma$ widths we need to choose iota couplings rather precisely in order to exploit the sensitivity exhibited in these figures. This puts the couplings so near the point $D=0$ that we are now able to choose an alternative approach to solving the $2\gamma$ sum rules (27): we simply take the lesson from Figs. 21 and 22 that in the parameter range relevant to solutions having small $\iota\to K\bar{K}\pi$ branching ratio the two

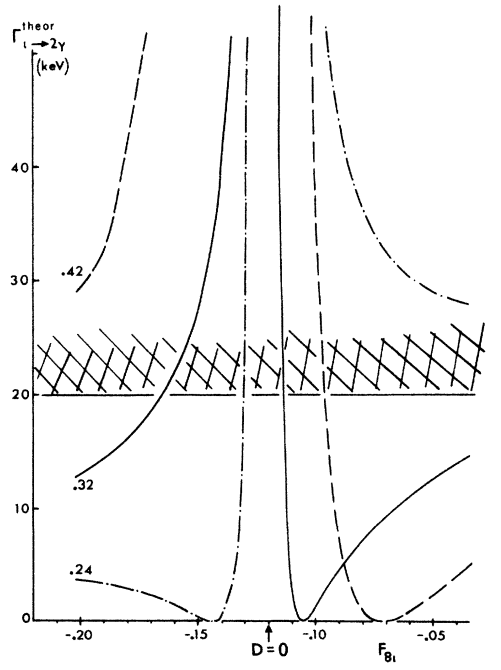


FIG. 22. Same as Fig. 21 but for $\iota\to 2\gamma$. The hatched region is excluded by the experimental upper bounds (Ref. 10) interpreted very conservatively as in the largest bound in Fig. 20.

$2\gamma$ sum rules (27) are no longer independent. This occurs when $D=0$, whereupon Eq. (51c) gives a unique relation between the iota couplings:

$$F_{8\iota}=\left[\frac{F_{8\eta'}}{F_{0\eta'}}\right]F_{0\iota}\ . \tag{55}$$

For consistency of the octet and singlet sum rules in (27) we then obtain a condition which gives the $\eta\to 2\gamma$ amplitude uniquely in terms of the couplings obtained from solving the WI:

$$r_\eta=\frac{(2\sqrt{2}F_{8\eta'}-F_{0\eta'})}{\sqrt{3}(F_{0\eta}F_{8\eta'}-F_{8\eta}F_{0\eta'})}\ . \tag{56}$$

The remaining sum rule then follows:

$$r_{\eta'}+r_\iota\left[\frac{F_{0\iota}}{F_{0\eta'}}\right]=\frac{F_{0\eta'}(F_{0\eta}-2\sqrt{2}F_{8\eta})}{\sqrt{3}(F_{0\eta}F_{8\eta'}-F_{8\eta}F_{0\eta'})}$$
$$\underset{\text{limit}}{\overset{\text{SU(3)}}{\to}}2\frac{\sqrt{2}}{\sqrt{3}}\simeq 1.64\ . \tag{57}$$

The method of solution is now a simple modification of that used before: the usual input parameters are chosen but now one, $F_{8\iota}$, is varied until the condition $D=0$, Eq. (55), is satisfied. The result is plotted in Fig. 23 where we see that $F_{8\iota}$ spans only a narrow range about $F_{8\iota}=-0.12$. Supplied with the resulting solution to the WI we have all the couplings to evaluate Eqs. (56) and (57) which are depicted in Figs. 24 and 25. Clearly an acceptable fit to all the experimental restrictions is possible *provided* a small $\iota\to K\bar{K}\pi$ branching ratio less than 50% is considered viable. It seems only possible to achieve a large enough branching ratio by either violating SU(3) symmetry badly (for the $\eta$ and $\eta'$ couplings) or by going toward the previously discussed solution with suppressed singlet iota coupling $F_{0\iota}$.

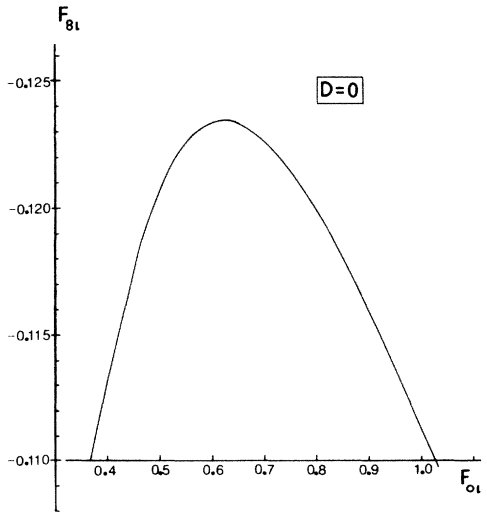


FIG. 23. Values of $F_{8\iota}$ satisfying the condition $D=0$ in Eq. (55). Input parameter values are $X_{0T}=1.9$ and $\chi_t=0$ (corresponding to $A_\iota=0.44$).

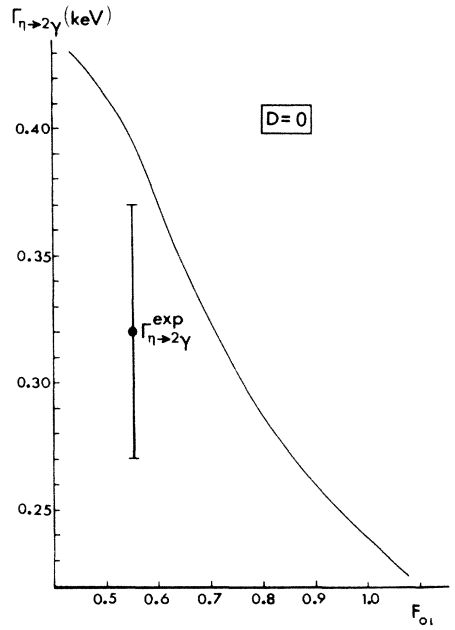


FIG. 24. Width for $\eta\to 2\gamma$ as given by the condition $D=0$. Values of $F_{0\iota}$ now uniquely determine $F_{8\iota}$ which varies by no more than 5% from the value $F_{8\iota}=-0.12$ over the range of $F_{0\iota}$ depicted here—see Fig. 23. We have taken $X_{0T}=1.9$ and $\chi_t$, $\chi_t=0$ ($A_\iota=0.44$).

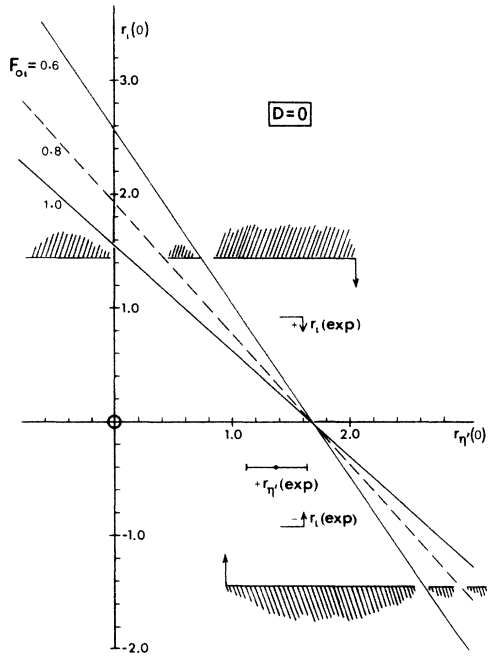


FIG. 25. Correlation between $2\gamma$ *amplitudes* for the case $D=0$ for three choices of $F_{0\iota}$. The corresponding $\eta$ width may be read off from Fig. 24 and we have taken $X_{0T}=1.9$, $\chi_t=0$ ($A_\iota=0.44$). The experimentally excluded region is again shown as in Fig. 20. Note that only positive values of $r_\eta$ are compatible, but either sign of $r_\iota$ is allowed—compare Fig. 20. The $r_{\eta'}$ intercept agrees well with the SU(3) limit in Eq. (57).

## X. DISCUSSION AND CONCLUSIONS

We have shown that the combined restrictions of maximal SU(3) symmetry and positive topological susceptibility make it possible to narrow down the range of phenomenologically viable solutions to only two: the one corresponds to a suppressed singlet iota coupling perhaps indicative of either a $\bar{q}q$ radial excitation or a glueball; the other to a more conventional singlet indicative of a $\bar{q}q$ meson like the $\eta'$. The former gives a large ratio $R_{\eta'/\iota}$ unlikely for a glueball $\iota$, but which is favored by the experimental dominance of the $\iota \to K\bar{K}\pi$ channel; the latter to a much smaller value requiring a branching ratio considerably smaller than is currently favored by experiments. It is important to note that the singling out of a small region of parameter space was achieved virtually independently of the 2 $\gamma$ decay restrictions: these were used more as a consistency check and it is quite encouraging that such viable values actually emerge in Figs. 20 and 25. It is of course possible to weaken our SU(3)-symmetry restrictions and obtain viable solutions between the two discussed here thereby making the distinction between possible solutions less clear-cut. But we could only accomplish this by allowing for a smaller ratio $R_{\eta'/\iota}$ corresponding to a small $\iota \to K\bar{K}\pi$ branching ratio not favored by current experiments. The size of this branching ratio is therefore important both here and in other discussions of the iota[2,18] and we await further experimental clarification with some interest.

Further interest resides in a better upper bound to or even a direct measurement of the $\iota \to 2\gamma$ width. All the indications of this analysis are that this width is small,[12–15] and a confirmation of this would greatly enhance our faith in the usefulness of the PCAC-anomaly sum rules (27) upon which these predictions are based. The reason why these sum rules need an iota width less than 10 keV is not hard to see: with SU(3) symmetry for the $\eta$ and $\eta'$ couplings the sum rules are near saturation with their contributions alone; and with iota couplings in the range of our two classes of solution the maximum value for the amplitude $r_\iota$ is of order $1F_\pi^{-1}$ leading to a width of order 9.5 keV. An inspection of Figs. 20 and 25 shows that the actual range of parameter values favored by our analysis tends to enhance this tendency in the direction of even lower values if the $\eta$ and $\eta'$ widths are to come out right: thus if we are optimistic about the complications of large extrapolations to the mass shell we see a strong tendency toward a width of at most 5 keV with a most favored value of approximately 2 keV for both types of solution. One reason for optimism regarding estimates or the $2\gamma$ widths is that they have been calculated in terms of the $\eta$ width via sum rules rather than absolutely and these may have a much wider range of validity than just $q^2=0$.

Another interesting point concerns the signs of the $2\gamma$ amplitudes discussed at length in the Appendix: both the solutions unambiguously predict that $r_{\eta'}$ has the same sign as $r_\eta$, a result consistent with the Steinberger[10]

TABLE I. Representative solutions to the anomalous Ward identities. Some solutions to the WI's which illustrate the two classes of solution found. The no-$\iota$ solution (Ref. 5) is shown for comparison. Solutions I and II correspond to "suppressed" iota singlet coupling $F_{0\iota}$; solution I is our favored one with the best compromise between the various requirements imposed in Sec. IX, and with $B(\iota \to K\bar{K}\pi)$ near 100%. SU(3) symmetry favors $\chi_t=0$; solution II shows the effect on solution I when the latter is increased to its maximum value. Note particularly the large SU(3) breaking in $F_{0\eta}$. Solutions III, IV, and V correspond to unsuppressed $F_{0\iota}=0.7$–$1.0$ and consequently small $B(\iota \to K\bar{K}\pi)$; in all three solutions $D=0$ [see Eqs. (55)–(57)].

| | no-$\iota$ | I | II | III | IV | V | Experimental value |
|---|---|---|---|---|---|---|---|
| $F_{8\eta}$ | 0.97 | 1.01 | 1.01 | 1.08 | 1.10 | 1.11 | |
| $F_{8\eta'}$ | −0.35 | −0.13 | −0.13 | −0.16 | −0.14 | −0.10 | |
| $F_{8\iota}$ | | −0.20 | −0.22 | −0.12 | −0.12 | −0.11 | |
| $F_{0\eta}$ | 0.38 | 0.14 | 0.33 | 0.11 | 0.11 | 0.12 | |
| $F_{0\eta'}$ | 1.18 | 0.91 | 0.90 | 0.91 | 0.91 | 0.91 | |
| $F_{0\iota}$ | | 0.50 | 0.65 | 0.70 | 0.80 | 1.00 | |
| $A_\eta$ | 1.01 | 0.87 | 0.99 | 0.83 | 0.84 | 0.86 | |
| $A_{\eta'}$ | 0.91 | 0.70 | 0.79 | 0.66 | 0.67 | 0.69 | |
| $A_\iota$ | | 0.44 | 0.51 | 0.68 | 0.78 | 0.97 | |
| $6\chi_t$ | 1.35 | 0 | 1.36 | 0 | 0 | 0 | |
| $6\chi_t^0$ | 57.5 | 55.2 | 73.6 | 80.8 | 96.7 | 135.1 | |
| $R_{\eta'/\eta}$ | 0.9 | 0.8 | 0.8 | 0.8 | 0.8 | 0.8 | 0.8±0.1 |
| $R_{\eta'/\iota}$ | | 1.59 | 1.57 | 0.98 | 0.87 | 0.71 | $(1.68\pm0.36)[B(\iota \to K\bar{K}\pi)]^{1/2}$ |
| $B(\iota \to K\bar{K}\pi)$ | | (90%) | (87%) | (34%) | (27%) | (18%) | |
| $\Gamma_{\eta\to 2\gamma}$ (keV) | 0.49 | 0.36 | 0.32 | 0.32 | 0.29 | 0.24 | 0.32±0.05 |
| $\Gamma_{\eta'\to 2\gamma}$ (keV) | 3.1 | 6.1 | 5.7 | 5.5 | 5.5 | 5.5 | 5.3±1.6 |
| $\Gamma_{\iota\to 2\gamma}$ (keV) | | 1.1 | 0.2 | 1.3 | 1.1 | 0.7 | $<10$ (keV) |

baryon triangle and one which in principle may be subjected to experimental test in $\eta'$ photoproduction. There are further tests of solution signs but these are almost certainly beyond the bounds of any foreseeable experiments. It is also surprising that there remains only a twofold sign ambiguity in our solutions as a result of the analysis in the Appendix: these correspond to the signs given for the solutions presented explicitly here (solutions 1A of the Appendix) and numerically identical solutions with reversed signs for all the *iota* couplings (solution 1B of the Appendix).

The figures presented in this paper are meant to serve as both a convenient summary of the results and a realistic indication of the sensitivity and mutual interdependence of the relevant parameters of the $\eta$-$\eta'$-$\iota$ system. We conclude with Table I which shows a selection of typical parameter values and compare these with ones obtained in a similar analysis neglecting the iota.[5] We regard this investigation mainly as a preliminary to a better-controlled and more fundamental approach to the nonperturbative consequences of QCD and hope to have provided a point of comparison for these calculations of the future. The limitations of our model to only one higher state, the $\iota(1440)$, means that our conclusions probably refer to the collective effects of important states above 1.4 GeV rather than to the $\iota$ alone. In particular, we have shown that the $\iota(1440)$ and so far unobserved $\bar{q}q$ radial excitations must play a role in elucidating the pseudoscalars and the QCD vacuum. This "effective" $\iota$ seems to possess a suppressed axial singlet coupling which, taken with a large ratio $R_{\eta'/\iota}$, points toward a radially excited state rather than a glueball or ground state $\bar{q}q$ like the $\eta'$. The presence of the $\iota(1440)$ also affects the value of the total topological susceptibility $\chi_t$ (Fig. 3) for which a small value seems to be favored; indeed it appears possible to achieve $\chi_t \approx 0$. Is this an indication of some dynamical mechanism at work corresponding to the resolution of the strong *CP*-violation problem? There is already some evidence of small $\chi_t$ coming from QCD sum rules[18c] and we look forward to the time when lattice simulations[6] gain the sophistication to handle fermions, topology, and glueballs all together. So far lattice calculations in this area work only in the no-quark limit for which our results on $\chi_t^0$ ($\approx \chi_t^{\rm YM}$) should be relevant: Fig. 6 and the discussion in Sec. III show that there may be a considerable enhancement of the "no quarks" topological susceptibility over that expected from previous $\iota$-less analyses.[4,5] Sections VII and VIII provide some succinct formulas for the topological susceptibility which may be useful as a guide especially as they depend on so few of the additional details required to obtain values for the axial couplings; this point is particularly noted in Sec. VII.

Finally there is the mixing problem: in principle the axial-vector couplings should contain information about the mixture of quarks and pure glueball in the $\eta$-$\eta'$-$\iota$ states, but we have not been able to exploit this so far.[5] It has not been necessary to invoke any particular mixing model in this work and although it is clear that additional input is required to make a comparison with the many mixing schemes already in existence,[23] it is not obvious how to do this.

## ACKNOWLEDGMENTS

I thank the following who have at various times provided advice, discussion and correspondence: B. Bagchi, D. J. Broadhurst, D. M. Capper, R. J. Crewther, R. B. Jones, D. G. Sutherland, and E. van Herwijnen.

## APPENDIX: RESOLVING SIGN AMBIGUITIES

The bilinear form of the WI (29) means that there are two independent sign ambiguities: one from the solution of (29a) denoted $\xi_8 = \pm 1$; the other from (29c) denoted $\xi_0$. These were chosen positive in the text but enter into the solutions (32) in the $x$-$y$-$\iota$ system as

$$\mathbf{X}_8 = \begin{pmatrix} \xi_8/b \\ 0 \\ X_{8\iota} \end{pmatrix}, \tag{A1}$$

$$\mathbf{X}_0 = \begin{pmatrix} \xi_8 a \\ \xi_0/c \\ X_{0\iota} \end{pmatrix}, \tag{A2}$$

$$\mathbf{Y} = \begin{pmatrix} -\xi_8 b X_{8\iota} Y_\iota \\ \xi_0 c\,[X_0^2 - 1 - Y_\iota (X_{0\iota} - X_{8\iota} a b)] \\ Y_\iota \end{pmatrix}, \tag{A3}$$

where

$$a \equiv b(\alpha - X_{0\iota} X_{8\iota}), \tag{A4}$$

$$b \equiv (1 - X_{8\iota}{}^2)^{-1/2}, \tag{A5}$$

and

$$c \equiv (X_{0T}{}^2 - a^2)^{-1/2}. \tag{A6}$$

Further sign ambiguities arise only at the next stage of the solution procedure when we need to rotate from the $x$-$y$-$\iota$ coordinate system to the physical $\eta$-$\eta'$-$\iota$ system: here we rotate about the $\iota$-axis by the angle $\phi$ given by

$$\tan\phi = \frac{rY_x - Y_y}{Y_x + rY_y}, \tag{A7}$$

where

$$r \equiv \frac{m_{\eta'}}{m_\eta} R_{\eta'/\eta} \approx \frac{m_{\eta'} A_{\eta'}}{m_\eta A_\eta}. \tag{A8}$$

The quantity $r$ is the first point in this sequence of equations where an experimentally measured quantity appears, and it may seem to be the appropriate observable relative to which all signs should be referred; but since there is no obvious way to experimentally measure the sign of $r$ relative to other relevant quantities such as $F_{\pi^0}$ and the strong interaction coupling $G_{\pi NN}$ we prefer instead to refer all signs to the $\eta \to 2\gamma$ amplitude $r_\eta$ which, at least in principle, has an experimentally measurable sign (relative to $G_{\pi NN}$). We shall discuss this point in detail at the end of this Appendix. We therefore have yet two more ambiguities: the sign of the amplitude ratio $r$ for

$\psi \to \eta'(\eta)\gamma$ and the twofold choice $\phi$ or $\phi+\pi$ corresponding to the sign reversal $(\sin\phi,\cos\phi)\to-(\sin\phi,\cos\phi)$ which leaves $\tan\phi$ unchanged. This latter sign reversal simply changes the sign of the $\eta$ and $\eta'$ components of the vectors (A1)—(A3) *after* rotation to the physical axes; but this sign change may also be accomplished by the reversal *before* rotation of $(\xi_8,\xi_0)\to-(\xi_8,\xi_0)$ and is therefore not an independent ambiguity: we are at liberty to always choose $|\phi|\leq\pi/2$.

The final result is a set of eight apparently independent solutions corresponding to the eightfold sign ambiguity in $\xi_8$, $\xi_0$, and $r$. These break up into just two sets which are *numerically* distinct; but the four solutions within each set differ from each other by sign permutations: the choice $(\xi_8,\xi_0,r)=(+,+,+)$ denoted solution 1 in Table II and those obtained from it by an even number of sign changes are all numerically identical and are called type-I solutions; solutions 5 with $(-,+,+)$ and all other odd sign changes of solution 1 are numerically identical to each other but differ from type I. These type I solutions are the nearly SU(3)-symmetric ones discussed in this paper and in Ref. 14 where only solution 1 is presented explicitly; type-II solutions all violate SU(3) symmetry by interchanging the SU(3) roles of $\eta$ and $\eta'$ (Ref. 5) and will not be considered further.

The proof that sets of solutions are numerically identical is straightforward and depends on the symmetries of the WI: in the form (29) and *in the physical* $\eta$-$\eta'$-$\iota$ *system* is it obvious that solutions related by the following sign changes are numerically identical:

$$(X_{8a},X_{0a},Y_a)\to-(X_{8a},X_{0a},Y_a)\ ,$$

i.e.,

$$(F_{8a},F_{0a},A_a)\to-(F_{8a},F_{0a},A_a) \tag{A9}$$

for $a=\eta$ and/or $\eta'$ and/or $\iota$. Ignoring for the moment changes in the iota couplings, each of the remaining three symmetry transformations on the $\eta,\eta'$ couplings occurs twice in Table II: once in transformations of solution 1; once in that of solution 5. There is no symmetry transformation between type I and type II: they are numerically distinct. The correspondence between transformations (A9) in the $\eta$-$\eta'$-$\iota$ system and sign changes in the $x$-$y$-$\iota$ system (implemented by sign changes of $\xi_8,\xi_0,r$) may be read off from the solutions (A1)—(A3) *after* rotation (37) by the angle $\phi$: these are listed in the fourth row of Table II.

The question of sign permutations in the iota couplings and the corresponding symmetries in (A9) must be seen in the context of the particular method used here to solve the WI's: these are taken as *input* parameters and a thorough search made in both the magnitudes and signs of these with $F_{0\iota}$ taken positive. Other choices of signs for $F_{8\iota}$ and $A_\iota$ than those presented in this paper fail the tests listed in Sec. IX, particularly the SU(3) test. However there remains the symmetry (A9) corresponding to the possibility of reversing the signs of all the iota couplings *together*: the result is a doubling of the number of numerically indistinguishable solutions from four to eight with one set having $(F_{0\iota},F_{8\iota},A_\iota)=(+,-,+)$ giving type-IA and type-IIA solutions; the other $(-,+,-)$, type-IB and type-IIB solutions.

Finally we consider the eight apparently acceptable

TABLE II. Solutions to the *WI alone* have sign ambiguities which correspond to freedom for arbitrarily choosing the signs of quantities listed in the first three rows. The row below these lists the equivalent transformations in Eq. (A9): the first four columns are symmetry transformations of solution 1; the next four of solution 5. The "output" rows give the signs of relevant experimental amplitudes calculated from type-I solutions to the WI; those in the solution 1 column are taken from the favored solutions presented in the text. Output quantities denoted $(\neq)$ are numerically different from solution 1. Entries in square brackets are for solutions where all iota couplings undergo sign reversal according to (A9).

| | Type-I solutions | | | | Type-II solutions | | | |
|---|---|---|---|---|---|---|---|---|
| Solution | 1 | 2 | 3 | 4 | 5 | 6 | 7 | 8 |
| $\xi_8$ | + | − | + | − | − | + | − | + |
| $\xi_0$ | + | + | − | − | + | + | − | − |
| $r\propto R_{\eta'/\eta}$ | + | − | − | + | + | − | − | + |
| Equivalent symmetry transform | of solution 1 | $\eta$ | $\eta'$ | $\eta$ and $\eta'$ | of solution 5 | $\eta$ | $\eta'$ | $\eta$ and $\eta'$ |
| | | | | Output signs | | | | |
| $r_\eta$[a] | + | + | + | + | + | + | + | + |
| $r_{\eta'}$ | + [+] | $(\neq)$ [$\neq$] | − [−] | $(\neq)$ [$\neq$] | Not related to type-I solutions | | | |
| $r_\iota$ | + [−] | $(\neq)$ [$\neq$] | + [−] | $(\neq)$ [$\neq$] | | | | |
| $R_{\eta'/\iota}$ | + [−] | + [−] | − [+] | − [+] | | | | |

[a]Positive by convention: all signs measured relative to $r_\eta$.

solutions: four of type IA and four of type IB. Four of these may be eliminated because although they all correspond to *numerically* identical couplings they give very different and unacceptable values for the *output* $\eta'$ and $\iota\to 2\gamma$ widths; this is indicated in the last four rows of Table II. That not all type-I solutions give identical output is evident from Eqs. (51) which are numerically invariant only under sign changes of all the iota and all the $\eta'$ couplings, either together or separately as in (A9), but not under changes of the $\eta$ signs.

To summarize there are four acceptable solutions, numerically identical but distinguished by differing sign combinations for decay amplitudes:

$$(r_{\eta'},r_\iota \mid R_{\eta'/\eta},R_{\eta'/\iota})=\begin{cases}(+,+\mid +,+) & \text{solution 1A}\ ,\\ [+,-\mid +,-] & \text{solution 1B}\ ,\\ (-,+\mid -,-) & \text{solution 3A}\ ,\\ [-,-\mid -,+] & \text{solution 3B}\ .\end{cases} \tag{A10}$$

This brings us to the question: is there any physical difference between the remaining four apparently equally acceptable type-I solutions and can they be distinguished experimentally? Surprisingly this is not an unreasonable question because at least in principle the signs of pseudoscalar $2\gamma$ amplitudes $r_a$ relative to strong couplings $G_{aNN}$ may be measurable in pseudoscalar photoproduction at small angles through the interference between the direct channel (Reggeized) Born term and the cross-channel Primakoff photon-exchange diagram. This possibility was pointed out 15 years ago by Gilman[24] who used the data on $\pi^0$ photoproduction off protons to show that the observed constructive interference implied that $r_\pi$ has the opposite sign to $G_{\pi NN}$; this confirmed the earlier result obtained by Okubo[25] based on somewhat more theory-dependent arguments; but it also confirms the original Steinberger[10] calculation with a proton-loop which itself is equivalent to the quark-loop anomaly calculation when the Goldberger-Treiman relation is used. Although in principle we may attempt to apply the same method to the $\eta$, $\eta'$, and $\iota$ the experimental data is either not yet good enough or does not even exist. Instead, the following the success of the Steinberger prediction for the sign and magnitude of the $\pi^0\to 2\gamma$ amplitude we will assume that the appropriate baryon triangle diagrams are at the very least able to give the correct relative signs for the $\eta$, $\eta'$, and $\iota\to 2\gamma$ amplitudes. Since these amplitudes depend on the couplings of these pseudoscalars to baryons we will need additional assumptions—SU(3) symmetry and the quark model—to relate the signals to each other and then finally to the $\pi$-$N$ coupling.

Ignoring common positive factors we have, for the $\Pi_a\to 2\gamma$ amplitude from the baryon loop

$$r_a \propto -\frac{G_{aBB}}{M_B}\ , \tag{A11}$$

where the numerator is the pseudoscalar-baryon coupling, the denominator the baryon mass. For the $\pi$ this expression contains only the proton contribution (because neither $\pi$ nor proton contain $s$ quarks) and hence we obtain Gilman's result.[24] For the $\eta$ and $\eta'$ there are several complications: First there is mixing with the pure octet and singlet:

$$\eta=\eta_8\cos\theta-\eta_0\sin\theta,\quad \eta'=\eta_0\cos\theta+\eta_8\sin\theta\ , \tag{A12}$$

where the quark content of the pure SU(3) states is

$$\eta_8=\frac{1}{\sqrt{6}}(\bar{u}u+\bar{d}d-2\bar{s}s)\ ,$$
$$\eta_0=\frac{1}{\sqrt{3}}(\bar{u}u+\bar{d}d+\bar{s}s)\ . \tag{A13}$$

Since the proton only contains $u$ and $d$ quarks we obtain a simple relation between singlet and octet couplings:

$$G_{\eta_0 NN}=\sqrt{2}G_{\eta_8 NN}\ . \tag{A14}$$

Hence, using the mixing angle $\theta=-10°$ (Ref. 21) we obtain the physical particle couplings:

$$G_{\eta NN}=G_{\eta_8 NN}(\cos\theta-\sqrt{2}\sin\theta)=1.23G_{\eta_8 NN}\ ,$$
$$G_{\eta' NN}=G_{\eta_8 NN}(\sqrt{2}\cos\theta+\sin\theta)=1.22G_{\eta_8 NN}\ . \tag{A15}$$

Finally we assume SU(3) symmetry for the baryon octet-pseudoscalar octet coupling:

$$G_{\eta_8 NN}\approx\frac{1}{\sqrt{3}}(3-4\alpha)G_{\pi NN}\ , \tag{A16}$$

where $\alpha$ is the $D/(D+F)$ ratio. Determinations of the baryon octet couplings to the pseudoscalar octet[11] are consistent with a value

$$\alpha\approx 0.5\text{–}0.6 \tag{A17}$$

from which we obtain

$$G_{\eta NN}\approx G_{\eta' NN}\approx 0.5G_{\pi NN}\ . \tag{A18}$$

Since the signs are the same as each other and as the $\pi$-$N$ coupling we conclude that $r_\pi$, $r_\eta$, and $r_{\eta'}$ all have the same sign: negative relative to the $\pi$-$N$ coupling. Equation (A10) shows that the only solutions consistent with this result are 1A and 1B (recall that all signs so far have been quoted relative to $r_\eta$ taken positive by convention; to obtain them relative to $G_{\pi NN}$ requires a reversal of all signs quoted in the text). One possible complication which may alter our conclusion is that both the $\eta$ and $\eta'$ contain strange quarks so that we probably ought to take account of contributions to (A11) from the strange baryons $\Sigma$ and $\Xi$. We have examined these couplings using the same principles as above and find that the $\Xi$ couplings are the only ones which are negative for $\alpha$ values given by (A17); positive $\Sigma$ couplings tend to work against this making an overall sign change most unlikely. From the quark contents of the pure SU(3) states we obtain

$$G_{\eta_8\Xi\Xi}=\frac{\sqrt{3}}{\sqrt{2}}G_{\eta_0\Xi\Xi}$$

and

$$G_{\eta_8\Sigma\Sigma}=G_{\eta_0\Sigma\Sigma}\ . \tag{A19}$$

Using the pseudoscalar mixing angles, SU(3)-symmetric

baryon couplings and $\alpha \approx 0.5$ we obtain

$$\begin{aligned} G_{\eta\Xi\Xi} &\approx 1.13 G_{\eta_8\Xi\Xi} \approx -1.3 G_{\pi NN} , \\ G_{\eta'\Xi\Xi} &\approx 0.63 G_{\eta_8\Xi\Xi} \approx -0.7 G_{\pi NN} , \\ G_{\eta\Sigma\Sigma} &\approx 1.16 G_{\eta_8\Sigma\Sigma} \approx 0.7 G_{\pi NN} , \\ G_{\eta'\Sigma\Sigma} &\approx 0.81 G_{\eta_8\Sigma\Sigma} \approx 0.5 G_{\pi NN} . \end{aligned} \tag{A20}$$

Weighted with the $\Sigma$ and $\Xi$ masses as in (A11) we obtain the contribution summed over $N$, $\Sigma$, and $\Xi$:

$$r_\eta \propto -0.3 \frac{G_{\pi NN}}{M_N}, \quad r_{\eta'} \propto -0.6 \frac{G_{\pi NN}}{M_N} . \tag{A21}$$

It is interesting to note that the ratio $r_{\eta'}:r_\eta$ is nearly correct according to Eq. (28) but the overall magnitude is about a factor 2 too small.

It is unlikely that we will ever be in a position to distinguish between the remaining two solutions 1A and 1B which differ in overall sign for the iota couplings; but (A10) shows that since not all sign combinations of the $\psi \to \Pi_a \gamma$ amplitudes are represented in solutions 1A and 1B there is a specific prediction for these signs once that of $r_\iota$ is known. Thus, at least in principle, there is physical significance in the question of signs.


[1]D. L. Scharre *et al.*, Phys. Lett. **97B**, 329 (1980); C. Edwards *et al.*, Phys. Rev. Lett. **49**, 259 (1982); P. Jenni *et al.*, Phys. Rev. D **27**, 1031 (1983). See also the entry under $E(1420)$ and $\iota(1440)$ in Ref. 21.

[2]S. U. Chung *et al.*, Phys. Rev. Lett. **55**, 779 (1985); **55**, 2093(E) (1985). For a useful review of the theoretical status of $\iota(1440)$, see P. M. Fishbane and S. Meshkov, Comments Nucl. Part. Phys. **13**, 325 (1984). See also M. Frank *et al.*, Phys. Rev. D **32**, 2883 (1985).

[3]R. J. Crewther, Riv. Nuovo Cimento **2**, 63 (1979); G. A. Christos, Phys. Rep. **116**, 251 (1984). These reviews contain a complete list of references on the U(1) problem.

[4]G. Veneziano, Nucl. Phys. **B159**, 213 (1979); H. Goldberg, Phys. Rev. Lett. **44**, 363 (1980); P. Di Vecchia and G. Veneziano, Nucl. Phys. **B171**, 253 (1980); C. Rosenzweig, J. Schechter, and G. Trahern, Phys. Rev. D **21**, 3388 (1980); K. Kawarabayashi and N. Ohta, Nucl. Phys. **B175**, 477 (1980); R. Arnowitt and P. Nath, Phys. Rev. D **23**, 473 (1981); Nucl. Phys. **B209**, 234 (1982); **B209**, 251 (1982).

[5]E. van Herwijnen and P. G. Williams, Phys. Rev. D **24**, 240 (1981); Nucl. Phys. **B196**, 109 (1982).

[6]P. Woit, Phys. Rev. Lett. **51**, 638 (1983); Nucl. Phys. **B262**, 284 (1985); G. Bhanot *et al.*, *ibid.* **B230**, 291 (1984); Y. Iwasaki and T. Yoshie, Phys. Lett. **143B**, 449 (1984).

[7]P. di Vecchia *et al.*, Nucl. Phys. **B192**, 392 (1981); K. Ishikawa *et al.*, Phys. Lett. **128B**, 309 (1983).

[8]E. Witten, Nucl. Phys. **B156**, 269 (1979).

[9]B. Berg and A. Billoire, Nucl. Phys. **B226**, 405 (1983); Ph. de Forcrand *et al.*, Phys. Lett. **152B**, 107 (1985).

[10]J. Steinberger, Phys. Rev. **76**, 1180 (1949).

[11]O. Dumbrajs *et al.*, Nucl. Phys. **B216**, 277 (1983).

[12]C. Rosenzweig, A. Salomone, and J. Schechter, Phys. Rev. D **24**, 2545 (1981).

[13]K. A. Milton, W. F. Palmer, and S. S. Pinsky, Phys. Rev. D **27**, 202 (1983).

[14]P. G. Williams, Phys. Rev. D **29**, 1032 (1984).

[15]B. Bagchi and S. Debnath, Z. Phys. C **22**, 175 (1984).

[16]H. Pagels, Phys. Rep. **16C**, 219 (1975); P. G. Williams, Nuovo Cimento **79A**, 437 (1984).

[17]H. Leutwyler and M. Roos, Z. Phys. C **25**, 91 (1984).

[18](a) L. J. Reinders, H. R. Rubinstein, and S. Yazaki, Phys. Lett. **120B**, 209 (1983); (b) N. V. Kvasnikov and A. A. Pivovarov, Nuovo Cimento **81A**, 680 (1984); (c) S. Narison, CERN Report No. TH 3990, 1984 (unpublished); (d) B. Bagchi and S. Debnath, J. Phys. G (to be published). This is not intended to be a comprehensive list but merely representative of some more recent estimates.

[19]R. J. Crewther, Phys. Lett. **70B**, 349 (1977).

[20]K. Ishikawa *et al.*, Phys. Lett. **120B**, 387 (1983); M. Chanowitz and S. Sharpe, Nucl. Phys. **B222**, 211 (1983); C. Carlson *et al.*, Phys. Rev. D **27**, 1556 (1983).

[21]Particle Data Group, Rev. Mod. Phys. **56**, S1 (1984).

[22]Y. Kitazawa, Phys. Lett. **151B**, 165 (1985).

[23]N. Aizawa, Z. Maki, I. Imemura, and K. Yamamoto, Prog. Theor. Phys. **63**, 962 (1980); J. L. Rosner, Phys. Rev. D **27**, (1983). F. Caruso *et al.*, Z. Phys. C **30**, 493 (1986). This is not a complete list but further references may be traced from these papers. For an alternative approach to pseudoscalar mixing using weak PCAC, see M. D. Scadron, Phys. Rev. D **29**, 2076 (1984).

[24]F. J. Gilman, Phys. Rev. **184**, 1964 (1969).

[25]S. Okubo, Phys. Rev. **179**, 1629 (1968).